

AD-A115 516

AIR FORCE INST OF TECH WRIGHT-PATTERSON AFB OH SCH00--ETC F/G 20/9  
SOFT PHOTON EFFECTS ON VACUUM POWER FLOW.(U)  
DEC 81 O J MITCHELL, R J BLAHER

UNCLASSIFIED

AFIT/GE/EE/81D-12

NL

| 1 2 |

1 2 3 4 5 6 7 8 9 10 11 12

1 2 3 4 5 6 7 8 9 10 11 12

1 2 3 4 5 6 7 8 9 10 11 12

1 2 3 4 5 6 7 8 9 10 11 12

1 2 3 4 5 6 7 8 9 10 11 12

1 2 3 4 5 6 7 8 9 10 11 12

1 2 3 4 5 6 7 8 9 10 11 12

1 2 3 4 5 6 7 8 9 10 11 12

1 2 3 4 5 6 7 8 9 10 11 12

1 2 3 4 5 6 7 8 9 10 11 12

1 2 3 4 5 6 7 8 9 10 11 12

1 2 3 4 5 6 7 8 9 10 11 12

1 2 3 4 5 6 7 8 9 10 11 12

1 2 3 4 5 6 7 8 9 10 11 12

1 2 3 4 5 6 7 8 9 10 11 12

1 2 3 4 5 6 7 8 9 10 11 12

1 2 3 4 5 6 7 8 9 10 11 12

1 2 3 4 5 6 7 8 9 10 11 12

1 2 3 4 5 6 7 8 9 10 11 12

1 2 3 4 5 6 7 8 9 10 11 12

1 2 3 4 5 6 7 8 9 10 11 12

1 2 3 4 5 6 7 8 9 10 11 12

1 2 3 4 5 6 7 8 9 10 11 12

1 2 3 4 5 6 7 8 9 10 11 12

1 2 3 4 5 6 7 8 9 10 11 12

1 2 3 4 5 6 7 8 9 10 11 12

1 2 3 4 5 6 7 8 9 10 11 12

1 2 3 4 5 6 7 8 9 10 11 12

1 2 3 4 5 6 7 8 9 10 11 12

1 2 3 4 5 6 7 8 9 10 11 12

1 2 3 4 5 6 7 8 9 10 11 12

1 2 3 4 5 6 7 8 9 10 11 12

1 2 3 4 5 6 7 8 9 10 11 12

1 2 3 4 5 6 7 8 9 10 11 12

1 2 3 4 5 6 7 8 9 10 11 12

1 2 3 4 5 6 7 8 9 10 11 12

1 2 3 4 5 6 7 8 9 10 11 12

1 2 3 4 5 6 7 8 9 10 11 12

1 2 3 4 5 6 7 8 9 10 11 12

1 2 3 4 5 6 7 8 9 10 11 12

1 2 3 4 5 6 7 8 9 10 11 12

1 2 3 4 5 6 7 8 9 10 11 12

1 2 3 4 5 6 7 8 9 10 11 12

1 2 3 4 5 6 7 8 9 10 11 12

1 2 3 4 5 6 7 8 9 10 11 12

1 2 3 4 5 6 7 8 9 10 11 12

1 2 3 4 5 6 7 8 9 10 11 12

1 2 3 4 5 6 7 8 9 10 11 12

1 2 3 4 5 6 7 8 9 10 11 12

1 2 3 4 5 6 7 8 9 10 11 12

1 2 3 4 5 6 7 8 9 10 11 12

1 2 3 4 5 6 7 8 9 10 11 12

1 2 3 4 5 6 7 8 9 10 11 12

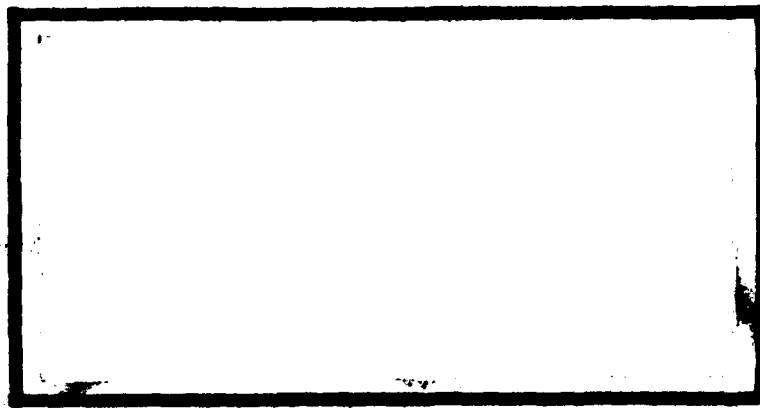
1 2 3 4 5 6 7 8 9 10 11 12

1 2 3 4 5 6 7 8 9 10 11 12

1 2 3 4 5 6 7 8 9 10 11 12

END  
DATE  
FEB 82  
DTIC

AD A113316



DTIC FILE COPY

DEPARTMENT OF THE AIR FORCE  
AIR UNIVERSITY (ATC)  
**AIR FORCE INSTITUTE OF TECHNOLOGY**

Wright-Patterson Air Force Base, Ohio

This document has been approved  
for public release and sale; its  
distribution is unlimited.

82 06 14 199

DTIC  
ELECTE  
S JUN 14 1982

E

AFIT/GE/EE/81D-12

1

SOFT PHOTON EFFECTS  
ON VACUUM POWER FLOW  
THESIS

AFIT/GE/EE/81D-12

Oakley J. Mitchell  
Captain USAF

Richard J. Blaher  
Captain USAF

DTIC  
RECEIVED  
JUN 14 1962

SOFT PHOTON EFFECTS  
ON VACUUM POWER FLOW

THESIS

Accession For	
NTIS GRA&I	<input checked="" type="checkbox"/>
DTIC TAB	<input type="checkbox"/>
Unannounced	<input type="checkbox"/>
Justification	
By _____	
Distribution/	
Availability Codes	
Avail and/or	
Dist	Special
A	

Presented to the Faculty of the School of Engineering  
of the Air Force Institute of Technology  
Air Training Command  
in Partial Fulfillment of the  
Requirements for the Degree of  
Master of Science



Oakley J. Mitchell, B.S., M.B.A.      by      Richard J. Blaher, B.S., M.S.  
Captain      USAF      Captain      USAF  
Graduate Electrical Engineering  
December 1981

Approved for public release; distribution unlimited

## Preface

The purpose of these experiments was to determine the effects of radiated energy, characterized by temperatures up to ten electron volts, on vacuum power flow. The experiments were undertaken to better understand vacuum power flow physics in support of the SHIVA test program at the Air Force Weapons Laboratory (AFWL).

We are most grateful to our adviser, Dr. Robert E. Reinovsky, for his patience during our learning experience. We are thankful for the time he took for impromptu sessions to explain principles and allow us to better understand concepts vital to the success of the experiments.

We would like to thank Captains Richard Henderson, Cecil Sturke, Mr. Brett Simpkins and Mr. Mark Coffing for their technical assistance on our respective experiments. We would also like to express our appreciation to all the support personnel at the Advance Concepts Branch, AFWL for their expert technical and administrative assistance.

Additionally, we would like to extend our gratitude to the P-1 Division of the Los Alamos National Laboratory, especially Dr. Don Kania and Dr. Clifford Woods who provided the diagnostic equipment and expert engineering advice necessary for the completion of these experiments.

Finally, we want to express our gratitude to our wives, Diana Blaher and Janis Mitchell, for their patience and encouragement throughout the project.

## Contents

	Page
Preface.....	ii
List of Figures.....	iv
List of Symbols.....	v
Abstract.....	vii
I. Introduction.....	1
II. Theory.....	5
Blackbody.....	5
Insulator Flashover.....	11
Gap Closure.....	17
III. Physical Description.....	19
Insulator Flashover.....	19
Gap Closure.....	25
Diagnostics.....	29
IV. Results.....	40
Insulator Flashover.....	40
Gap Closure.....	41
V. Discussion and Conclusions.....	45
Insulator Flashover.....	45
Gap Closure.....	47
VI. Recommendations.....	49
Insulator Flashover.....	49
Gap Closure.....	50
Bibliography.....	51
Vita: Captain Blaher.....	52
Vita: Captain Mitchell.....	53

## List of Figures

Figure	Page
1. Energy Density as a Function of Frequency.....	7
2. Spectral Emittance at Various Temperatures.....	9
3. Secondary Electron Emission Efficiency as Function of Energy...	12
4. Angle Between Insulator and Electric Field.....	13
5. Breakdown Voltage as Function of Insulator Angle.....	14
6. Vacuum Flashover Component Configuration.....	20
7. Radiation Temperature Versus Detector Ratio.....	23
8. Photo Diode Output Traces.....	23
9. Oscillograph Showing Insulator Flashover.....	24
10. Oscillograph Showing No Insulator Flashover.....	24
11. Modified SHIVA Chamber Cross-Section.....	27
12A. Copper Anode, Data Shot.....	28
12B. Copper Cathode, Data Shot.....	28
13. Vacuum Chamber Diagnostic Locations.....	30
14. Nitrogen Laser Coverage.....	31
15. Laser Shadowgram, Pre-Shot.....	32
16. Laser Shadowgram, Data Shot.....	33
17. X-ray Diode Cross-Section.....	35
18. X-ray Diode Circuit Configuration.....	35
19. Typical Rogowski Coil Signal.....	37
20. Typical $dv/dt$ Probe Signal.....	37
21. Streak Camera Photo.....	43
22. Percentage of Gap Closure.....	44
23. Blackbody Curve With Line Spectra.....	46
24. Quartz Window Transmittance.....	46

# List of Symbols

m	Meters
J	Joules
s	Seconds
w	Watts
P	Power, w
cm	Centimeters
v	Volts
I	Radiant Emittance, $w m^{-2}$
$\omega$	Frequency, Radians Per Second
k	Boltzman's Constant, $1.38 \times 10^{-23} J ^\circ K^{-1}$
T	Temperature, $^\circ K$
$\pi$	Pi, 3.14159
c	Speed of Light, $2.998 \times 10^8 m s^{-1}$
h	Planck's Constant, $6.663 \times 10^{-34} J s$
h	Constant, $1.0545 \times 10^{-34} J s$
W	Energy Density, $w m^{-2} u^{-1}$
$\sigma$	Stefan-Boltzmann Constant, $5.669 \times 10^{-8} w m^{-2} K^{-4}$
u, $\mu m$	$10^{-6} m$
$\lambda$	Wavelength, m
a	Constant, $2897 u ^\circ K$
A	Area, $m^2$
ev	Electron Volt
$\alpha$	Surface Charge Density
$\epsilon$	Electric Field, $v m^{-1}$
$\epsilon$	Constant, $8.854 \times 10^{-12}$ Farads Per Meter
$E_o$	Energy at Some Point on Insulator, ev



$E_i$	Energy at Unity Secondary Emission Rate, ev	
$\psi$	Angle Between Insulator and Electric Field, Degrees	
uf	$10^{-6}$	Farad
Kv	$10^3$	v
Ma	$10^6$	Amps
ns	$10^{-9}$	Seconds
rm	$10^{-9}$	Meters

Abstract

Understanding the physical processes of high power electrical energy transport is of major importance for the advancement of state-of-art directed energy, simulation, and confined fusion programs. Generation of high voltage, short duration pulses may result in high energy density plasma which produces quantities of vacuum ultra-violet (VUV) and soft X-ray photons in the range of 0.5-10 ev. Power transport down vacuum lines presents two problems which must be dealt with in every application--insulator flashover and electrode gap closure. The pulsed flashover and ablative closure mechanisms under soft VUV photon fluence are described. Two tests were conducted. First, an insulator surface was subjected to VUV photons (0.5 ev) using apertures of 0.0156 to 0.5 inches in diameter with and without a quartz window. The apertures had no effect in inhibiting a flashover; however, the quartz window prevented the occurrence of insulator flashover. Second, the gap closure rate of copper electrodes under the photon fluence of  $6 \times 10^9$  Watts per square meter was measured. A gap closure rate of 0.35 cm/microsecond was determined for the copper electrodes.

## I. INTRODUCTION

### Background

Vacuum power flow is the transport of very high power pulses through solid-vacuum interfaces and along vacuum-insulated transmission lines. Most applications of interest in which energy is delivered by high voltage, short duration pulses cannot be investigated at atmospheric pressure; thus, vacuum becomes the dielectric medium and must inhibit undesirable electric breakdown. Power flow is of major importance to the Department of Energy and the Department of Defense. The Department of Energy is interested in pulse power technology for inertial confinement fusion experiments. The Department of Defense is concerned with high energy transport in the development of nuclear weapon simulation techniques and a variety of advanced weapon concepts. Understanding the physical processes involved in high energy transport is important to the advancement of laser and particle beam technology and in x-ray simulation programs.

In general, a typical pulse power system consists of four major parts:

1. A source to provide the needed energy and form pulses.
2. A load such as plasma, gas, or a vacuum accelerator gap.
3. Conductors to connect the source to the load. High energy transport normally implies the use of transmission lines as the conducting medium.
4. A means of supporting the conductors and coupling the pulse to the load. Dielectric materials are often used for both functions.

Two general problems must be addressed in every power flow application. First, when an insulator is used in a vacuum, its ability to stand off voltage is severely limited on and near its surface. Bulk breakdown seldom occurs before a surface flashover because the surface strength of the insulator is only about one-tenth of the volume strength. Second, even if the insulator sustains the applied voltage, the possibility of breakdown between the conductors caused by electric field effects, ohmic heating effects, or plasma effects must be considered. Failure of either the interface or the gap between the conductors results in shunting of current and little or no power transfer to the load.

#### Problem and Scope

Significant work has been accomplished in understanding breakdown phenomena and the effects of a magnetic field at vacuum interfaces and in vacuum lines; however, little or no work has specifically addressed the behavior of vacuum power flow systems under the influence of strong vacuum-ultra-violet (VUV) and soft (1-10 ev) x-ray photons (Ref 1). In experiments which generate an ionized plasma, the radiated energy produced may be sufficient to initiate insulator flashover or failure of the interelectrode gap. The purpose of this thesis was to investigate the following two problem areas inherent in vacuum power flow under soft photon fluence:

1. Insulator Flashover: When a voltage is applied across an insulator, how is flashover (electric breakdown across the insulator) affected by photon fluence for photon energy between one-half and ten electron volts?

2. Gap Closure: What are the breakdown characteristics of a vacuum gap under the soft photon fluence for photon energy between one-half and ten electron volts?

#### Approach

The objective of the flashover experiment was to relate radiation energy and power incident on the insulator to physical processes involved in flashover. An experiment investigating surface flashover was conducted using polyethylene dielectric material. Exploded one-mil tungsten or aluminum wire was used as the radiation source.

The objective of the gap closure experiment was to characterize the motion of an ablative front as a function of radial position in the gap between two electrodes. The ablative front was produced when radiative energy impinging on the electrodes caused a thin layer of electrode material to vaporize, forming a plasma cloud which moved away from the surface. This effectively shortened the gap width and increased the probability of breakdown. A single power level was used, and the radiation source was an array of twelve five-mil aluminum wires.

Both the insulator flashover and gap closure are electrical breakdown phenomena which occur in a vacuum environment. If a wire filament is placed between conducting electrodes and then exploded, the wire produces radiation which impinges on the walls of a transmission line or on the surface of an insulator and initiates the breakdown mechanism. Data were collected during the breakdown and later analyzed. The ablative closure and surface flashover experiments were conducted in parallel. Data were examined throughout the investigation, and inconsistent data were checked where possible.

by repeating the related experiment. These experiments assessed only the effects of radiation on gap closure and dielectric flashover. A detailed description of all physical processes involved was not attempted.

Section I is an introduction. Section II reviews the theory of blackbody radiation to give order of magnitude estimates of energy and power. Vaporization and photo-electron emission are examined as the prominent mechanisms affecting both surface breakdown and gap closure. Section III describes the experimental setup. A hardware description is given and experimental methodology is explained. Section IV examines the results obtained and Section V gives conclusions that were made. Finally, Section VI discusses the implications of the experiments and recommends future work.

## II. THEORY

Because the radiation sources used in these experiments are characterized as blackbodies, an understanding of elementary blackbody theory as well as insulator flashover and gap closure principles is required. This section describes characteristics of blackbodies and develops a first order approximation for determining the temperature in electron volts of a given radiator. Then factors affecting insulator flashover are described and secondary electron emission on an insulator surface is examined. Finally, the gap closure problem is detailed and an approximation of the expected closure rate is given.

### Blackbodies

Every physical body which has a temperature higher than zero degrees Kelvin emits radiation due to its own temperature. When radiation is incident on a homogenous body, a fraction of the radiation is reflected, and the remainder penetrates the body and is either absorbed or transmitted. Radiation sources may be generally classified as "optically thin" or "optically thick." A thin source is one in which, on the average, radiation from the inner regions of the object reaches the surface unimpeded. An optically thick source radiates only from its surface. In other words, incident radiation cannot be transmitted through an optically thick body.

A blackbody is an optically thick radiator of uniform temperature which radiates in a manner characteristic of that temperature. For a temperature of zero degrees Kelvin the blackbody radiates nothing. It absorbs all incident radiation and appears black. The blackbody is

assumed to perfectly absorb radiation of all wavelengths and at all angles of incidence. As a perfect absorber, it serves as a standard with which real absorbers can be compared. The blackbody also emits the maximum radiant energy per unit surface area at a given temperature and, hence, serves as an ideal standard of comparison for a body emitting radiation. The total radiant energy emitted by a blackbody in a vacuum is a function only of its temperature. Hence, neither the characteristics of the surroundings nor the detail of the internal structure of the emitter effect the emissive behavior of the blackbody, which makes it particularly desirable for analytical description in vacuum power flow experiments.

Modern physics has demonstrated that radiation displays a dual character. Under the influence of physical or chemical processes radiant energy may be absorbed or released by atoms or molecules. Energy is released in small quantum packets, or photons, which travel at the speed of light along straight paths until they interact with another material. During their travel these photons exhibit wavelike characteristics. The emitted radiation is a result of internal oscillation-like motion of atoms and molecules.

The Rayleigh-Jeans equation,

$$I(\omega) = \frac{\omega^2 kT}{\pi^2 c^2} \quad (1)$$

predicts the spectral distribution of a blackbody radiator. This radiation was derived using a classical theory of physics. cursory examination quickly reveals a disparity. The amount of emitted light



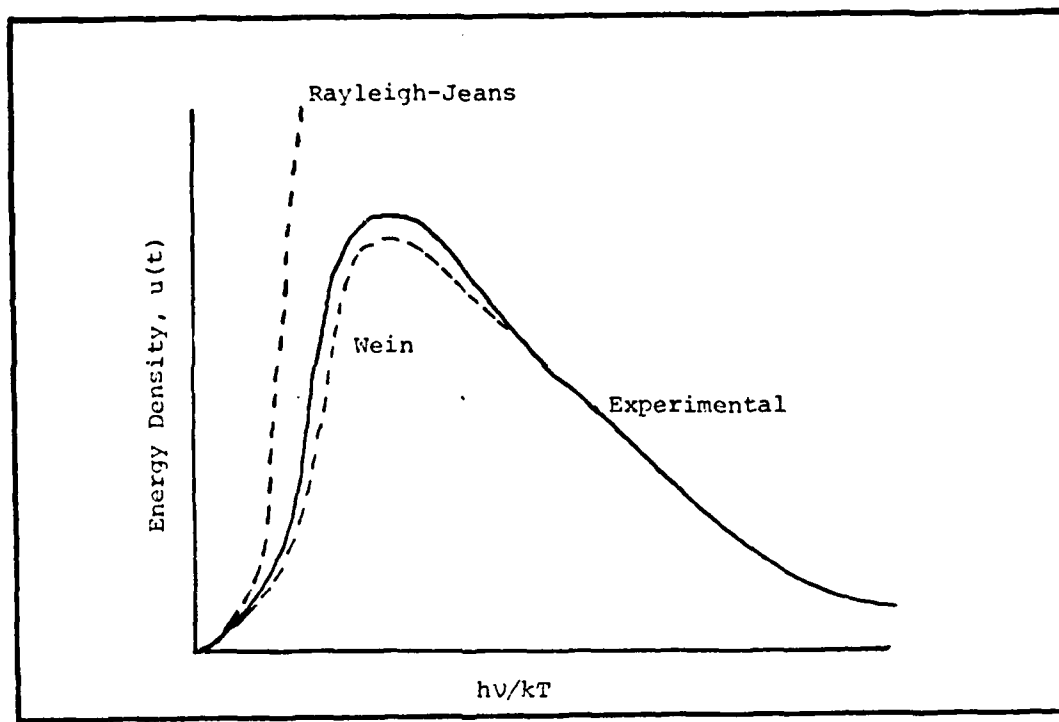


Figure 1. Energy Density as a Function of Frequency

increases as the square of frequency—without bound! This cannot be, and thus, the classical theory is insufficient for describing the spectral behavior of a blackbody. The problem is an assumption that the oscillator modes have unrestricted (continuous) frequencies. For very low frequencies, Equation (1) indeed fits the empirical energy density curve, as shown in Figure 1. Wein made observations at higher frequencies and suggested the equation

$$I(\omega)d\omega = \omega^3 e^{-h\omega/kT} d\omega \quad (2)$$

which fit the blackbody curve at higher frequencies, but was in error at low frequencies.

Planck studied the curve and arrived at an answer to the problem by approaching it from the back door. He first determined that

$$I(\omega) d\omega = \frac{\hbar \omega^3 d\omega}{\pi^2 c^2 (e^{\hbar\omega/kT} - 1)} \quad (3)$$

fit the curve nicely throughout the frequency spectrum. Then he proceeded to make up a set of rules to validate his equation. His major assumption was that the available energy occurs in photon packets which are equally spaced  $\hbar\omega$  apart. Detailed derivation of Equation (3) is beyond the scope of this report; however, in spite of the light treatment here, Planck's relation accurately depicts the empirical energy density curve in Figure 1. Even though there is a cubic factor in the numerator, the exponential function in the denominator increases at a faster rate and bends the curve back toward the axis.

The radiant flux emitted by a blackbody is obtained by multiplying the energy density by the speed of light. This quantity is the power per unit photon energy per unit area of the radiator. Integrating Equation (3) yields the total power radiated per unit area of the blackbody. The resultant expression for the radiant emittance, known as the Stefan-Boltzman Law, is

$$W = \frac{2\pi^5 k^4 T^4}{15c^2 h^2} = \sigma T^4 \quad (4)$$

The blackbody, compared to other geometrically equivalent thermal radiators of the same temperature, emits the maximum possible energy in all directions and at all wavelengths.

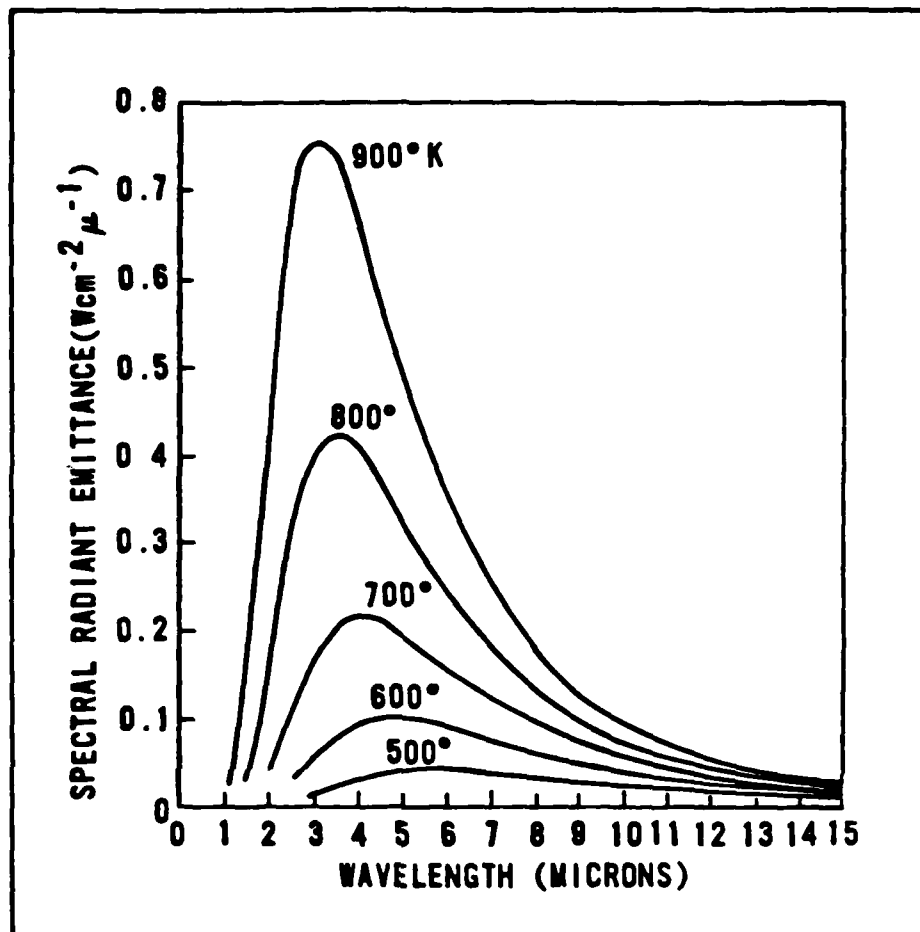


Figure 2. Spectral Emittance at Various Temperatures

In Figure 2 the spectral emittance curves for a typical blackbody are given. Some important characteristics of blackbodies are readily apparent from these curves. The emittance increases rapidly with temperature, as shown also in Equation (4). As an object is heated the predominant radiation wavelengths decrease proportionately. Finally, an obvious but important point is that the curves are continuous and never intersect; thus, for a higher temperature the radiant emittance is greater at all wavelengths. For any given temperature the maximum emittance occurs at some specific wavelength.

The wavelength can be determined from Wein's displacement law.

$$\lambda_m T = a \quad (5)$$

The blackbody radiation laws are particularly useful for determining power and energy in vacuum power flow experiments. For example, given a 5 ev cylindrical blackbody radiator which is 2 centimeters high and 0.635 centimeters in diameter, the radiant power per unit area is determined using Equation (4). Since T is given in electron volts, the conversion factor

$$1 \text{ ev} = 11605 \text{ }^\circ\text{K} \quad (6)$$

must be used to obtain a temperature of 58,025  $^\circ\text{K}$ . Substituting the temperature into the Stefan-Boltzman equation yields a power density of  $6.427 \times 10^{12} \text{ W m}^{-2}$ . The area of the cylindrical radiator is  $0.0008 \text{ m}^2$  and the energy flux emitted by the radiator is given by

$$P = \sigma T^4 A \quad (7)$$

and for this example is  $5.129 \times 10^8$  watts.

If the flux is multiplied by the time of emission, the total emitted energy can be obtained. For a typical emission time of 100 nanoseconds the delivered energy in this example would be 51.28 joules. The spectral distribution and power density can easily be determined with the given information. With a temperature of 5 ev, a radiant power density of  $8.45 \times 10^{12} \text{ W m}^{-2} \text{ u}^{-1}$  is obtained.

The blackbody radiation laws are used extensively in plasma experiments. A plasma is an ensemble of particles which acts

collectively and maintains a significant ionization potential. An optically thick plasma, one in which the plasma dimensions are much greater than the mean free path length of a photon, will absorb free photons readily; thus, such a plasma may be treated as a blackbody, and the simple calculations shown in the example may be used to accumulate abundant data about the radiative properties of the plasma. Because they are optically thick, the plasmas generated in the flashover and gap closure experiments are treated as blackbodies.

#### Insulator Flashover

Vacuum power flow requires insulation of a high voltage transmission line as it passes through the wall of a vacuum chamber, or construction of the chamber itself of dielectric material. Support of the transmission line within the vacuum chamber is also often accomplished with dielectric spacers. High voltage electric breakdown at vacuum-insulator interfaces is an important problem in a number of pulse power applications, particularly where high voltage and short rise times are required to deliver high power to the load. If the electrodes in a vacuum are separated by a solid insulating material, a spontaneous discharge may occur on or near the insulator surface of the dielectric. The voltage required to initiate the flashover is much lower than would be needed for bulk breakdown through the insulator, or flashover of the vacuum gap with the insulator removed; therefore, surface flashover is a major limiting factor in the operation of vacuum insulated systems. The sequence of events leading to breakdown and the physics involved have been investigated extensively but are not yet clearly understood.

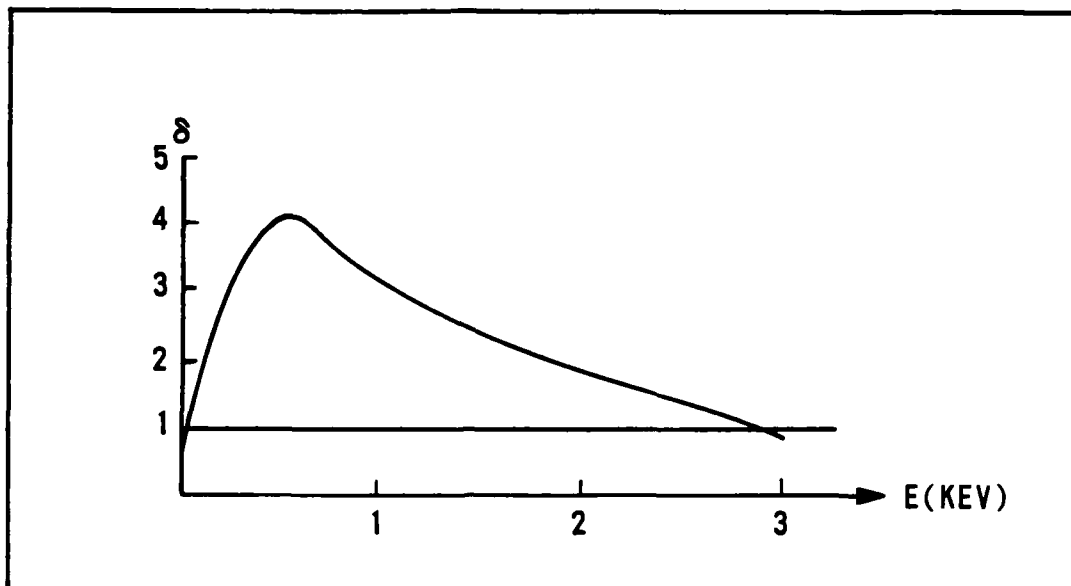


Figure 3. Secondary Electron Emission Efficiency as Function of Energy

It is well known that an insulator surface subjected to a high voltage can acquire a significant positive charge. One theory for the charging process is the theory of secondary electron emission (Ref 2:3073-3075). This theory postulates that field emission of electrons at the cathode-insulator-vacuum junction and insulator charging are involved in surface flashover. Field emitted electrons impact the insulator surface with enough energy to eject secondary electrons. The secondary emission results in a net positive charge left on the surface which becomes large enough to draw the secondary electrons back to the surface, setting up an avalanche condition. The probability of secondary electron release depends on the incident energy of returning electrons. It is also influenced by the insulator material surface texture and contamination. Figure 3 is a typical curve of the probability of secondary electron emission efficiency as a function of the energy of the impinging electrons. There are

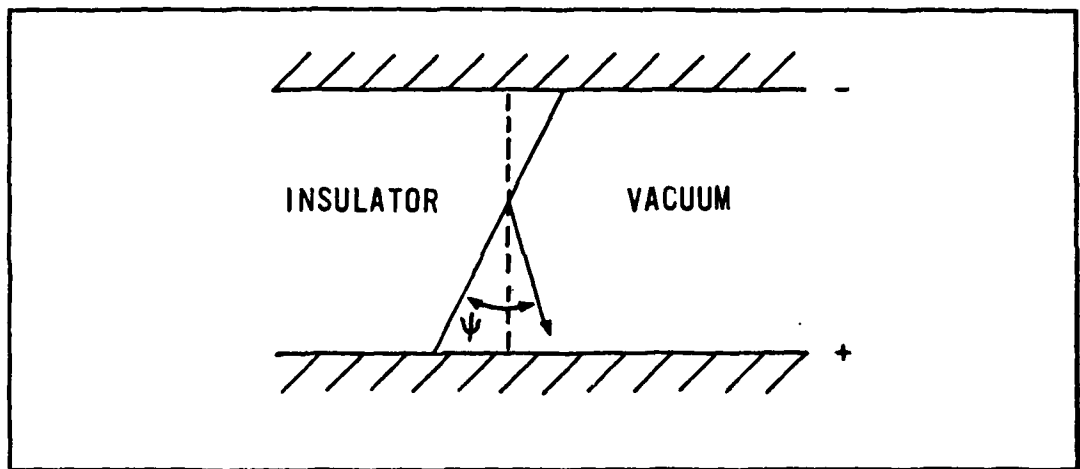


Figure 4. Angle Between Insulator and Electric Field

two points at which the energy yield is unity; that is, one impinging electron produces one secondary electron. Between these points the energy yield is greater than unity, and several secondary electrons may be released. The released electrons experience an energy gain due to the interelectrode field and are ultimately drawn back to the surface. The secondary electrons thus continue the production of additional secondaries on impact. Because of the average electric field in the vacuum gap, their trajectory is toward the anode, and the avalanche progresses until breakdown occurs.

When secondary electrons are emitted from the insulator, the surface becomes positively charged. The surface charge density, accounting for dielectric polarization, is

$$\alpha = 2\epsilon_0\epsilon_o \left[ \frac{1}{2} \left( \frac{E_i}{E_o} - 1 \right) \right]^{-1/2} \left[ \cos\psi - \left[ \frac{1}{2} \left( \frac{E_i}{E_o} - 1 \right) \right]^{1/2} \sin\psi \right] \quad (8)$$

Figure 4 depicts the angle  $\psi$ . This figure and Equation 8 show that, for a given dielectric material and interelectrode field, the

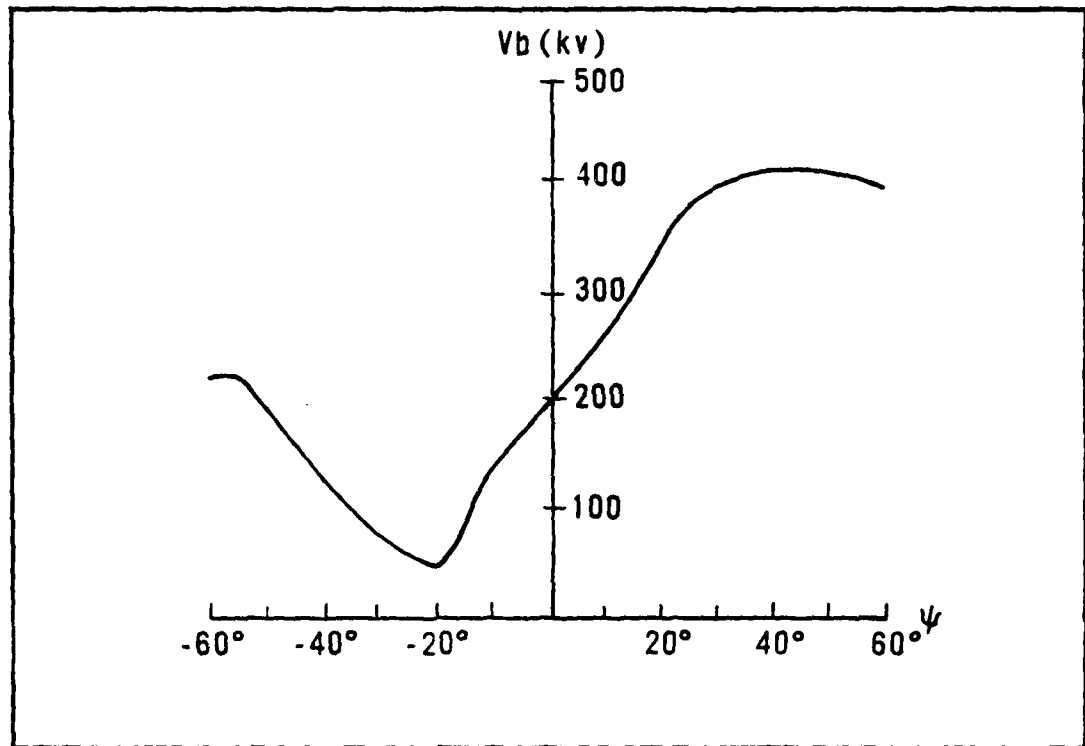


Figure 5. Breakdown Voltage as Function of Insulator Angle

surface charge density on a cylindrical insulator is greater than on a conical one (Ref 9:18). Thus, there is an extremely strong dependence on the angle between the insulator and the interelectrode field. Figure 5 shows the breakdown voltage and angle relationship for a typical insulator material (Ref 3:14). As the angle increases positively the flashover voltage increases also, and reaches a maximum. Milton noted that the maximum holdoff voltage was normally attained at an insulator angle near  $45^\circ$  to the interelectrode field (Ref 3:12-14). As the angle is varied in the negative direction similar phenomena occur; however, the maximum flashover voltage attainable is lower than that in the positive angle case.

The avalanche breakdown mechanism may be initiated by other than



field emission processes from the cathode. Radiative energy impinging on the insulator can be sufficient to cause electrons to separate from the surface. For a given insulator some threshold exists at which an incident photon will produce one or more secondary electrons to initiate or enhance the avalanche condition. A threshold value in terms of wavelength may readily be calculated. The ionization potential for polyethylene dielectric material is approximately 10 ev. The wavelength at this energy level is given by Equation (9).

$$\frac{12398.52}{10 \text{ ev}} = 1239.852 \text{ \AA} \quad (9)$$

Thus, recalling from Figure 2 that the power density of a blackbody is a function of wavelength, photons at wavelengths greater than about 1240 Angstroms would be expected to produce secondary electrons at the insulator. At longer wavelengths these photons would be expected to have little or no effect.

While the theory of secondary electron emission certainly provides a plausible explanation for the breakdown mechanism, it should be noted that no theory of the flashover mechanism has been unequivocally established. In the presence of radiant energy, incident photons may play a primary role in the production and multiplication of electrons leading to avalanche breakdown. Many variations of the hypothesis are possible and there most probably are other breakdown mechanisms which come into play.

Another factor which may be important in the breakdown process is the role of plasma near the insulator surface. Electron emission and subsequent deposition on the surface may produce sufficient energy to

heat and vaporize the insulator material. Radiation may also cause vaporization of a substantial amount of material near the insulator surface. Once vaporized the material can continue to absorb radiant energy and increase in temperature. When the resultant plasma density and temperature reaches some threshold, electrical breakdown occurs through the plasma. The current carried by the plasma rapidly develops into a low resistance discharge, aided by ablation of the insulator surface.

Certain physical characteristics of the equipment also play a role that affects the surface breakdown strength of an insulator. These include conditioning, insulator material, shape and surface condition of the insulator, and the angle that the insulator makes with the interelectrode field.

High voltage conditioning is a process by which progressively higher voltages are applied in steps across the insulator. With successive applications the breakdown potential follows a trend toward higher values. The incremental increase diminishes until a plateau is reached after which further increases in voltage yield no further improvement.

The breakdown voltage was shown by Milton and Gleichauf to be a function of insulator material (Ref 3,4,5). The flashover potential was found to be inversely proportional to the dielectric constant of the material (Ref 2). This might lead to a false assumption that selection of a material with a very low dielectric constant would eliminate the flashover problem. However, using a material with a low dielectric constant increases the probability of bulk breakdown

through the body of the insulator, and the trade-off is an important practical consideration. The breakdown voltage displays little evidence of electrode material dependence.

#### Gap Closure

In a vacuum gap closure may occur, and the vacuum insulation may fail when a radiation producing load is present in the gap. Radiation can heat surfaces sufficiently to generate gas and plasma from electrodes, vacuum transmission lines, and insulator surfaces. Ablated plasmas can move hydrodynamically and eventually bridge across the gap. The plasma temperature may increase sufficiently to produce a high-conductivity path and short circuit the gap, thus preventing energy transfer to the load. According to a study performed by Maxwell Laboratories, the plasma in the area near the load, where the radiation is the greatest, is hottest and most conductive (Ref 6:1-1). As the distance from the load increases, the plasma becomes colder and somewhat more resistive.

For a crude approximation the plasma load can be considered a "black" radiator. Consider a radiator having a 5 ev temperature for approximately 1 usec (Ref 7:1). The size of the radiator is the initial size of the load, 0.65 cm x 2 cm. A radiator having these parameters will emit 300 joules of energy at a power level of  $3 \times 10^8$  watts. This amount of radiated energy impinging on a copper electrode or transmission line can penetrate a few hundred angstroms into the material. Some energy will be lost by heat transfer due to conduction. This radiated energy, absorbed over a few square centimeters, will be consumed in a few (3-10) milligrams of copper. This absorption will produce a specific energy greater than 1 MJoule/gram, which is nearly

a hundred times greater than the vaporization specific energy of copper. The example serves to show that a substantial amount of material can be vaporized by this radiant energy. Once vaporized, the material continues to absorb energy which results in increased temperature and expansion of plasma into the vacuum gap. Gap closure rates of a few cm/usec are typical for this expansion(Ref 6,7).

### III. Physical Description

In this section a physical description of each respective experiment is given. Experiment, diagnostics, and experimental methodology are described. Variations in the insulator flashover experiment are described. The gap closure experiment diagnostics are described in detail because of the variety of equipment types used.

#### Vacuum Flashover

In the vacuum flashover experiment an insulator supporting a voltage,  $v$ , was placed in a vacuum environment. A wire was then exploded in the vicinity of the insulator to produce a radiation source. Voltage across the insulator was monitored to determine whether insulator flashover occurred and, if so, at what time.

Figure 6 is a diagram depicting the major components in the experiment. A six-inch diffusion pump was used to routinely achieve a pressure of  $1 \times 10^{-6}$  Torr in the vacuum chamber containing the insulator and radiation source. A high voltage supply, variable between 0-100 Kv, was used to charge a 5.6  $\mu\text{f}$  high density capacitor. The capacitor was discharged through the wire by triggering a mid-plane spark gap which was used to hold off the capacitor charge voltage until the desired firing time. The switch was pressurized with compressed air to keep the electrodes free of debris and prevent spontaneous breakdown of the spark gap. A charge of 26 Kv was adequate to cause vaporization of the wire and the use of higher voltages did not significantly affect either the apparent source temperature or insulator behavior. In the event of an abort or system malfunction the Jennings switch provided a discharge path for the

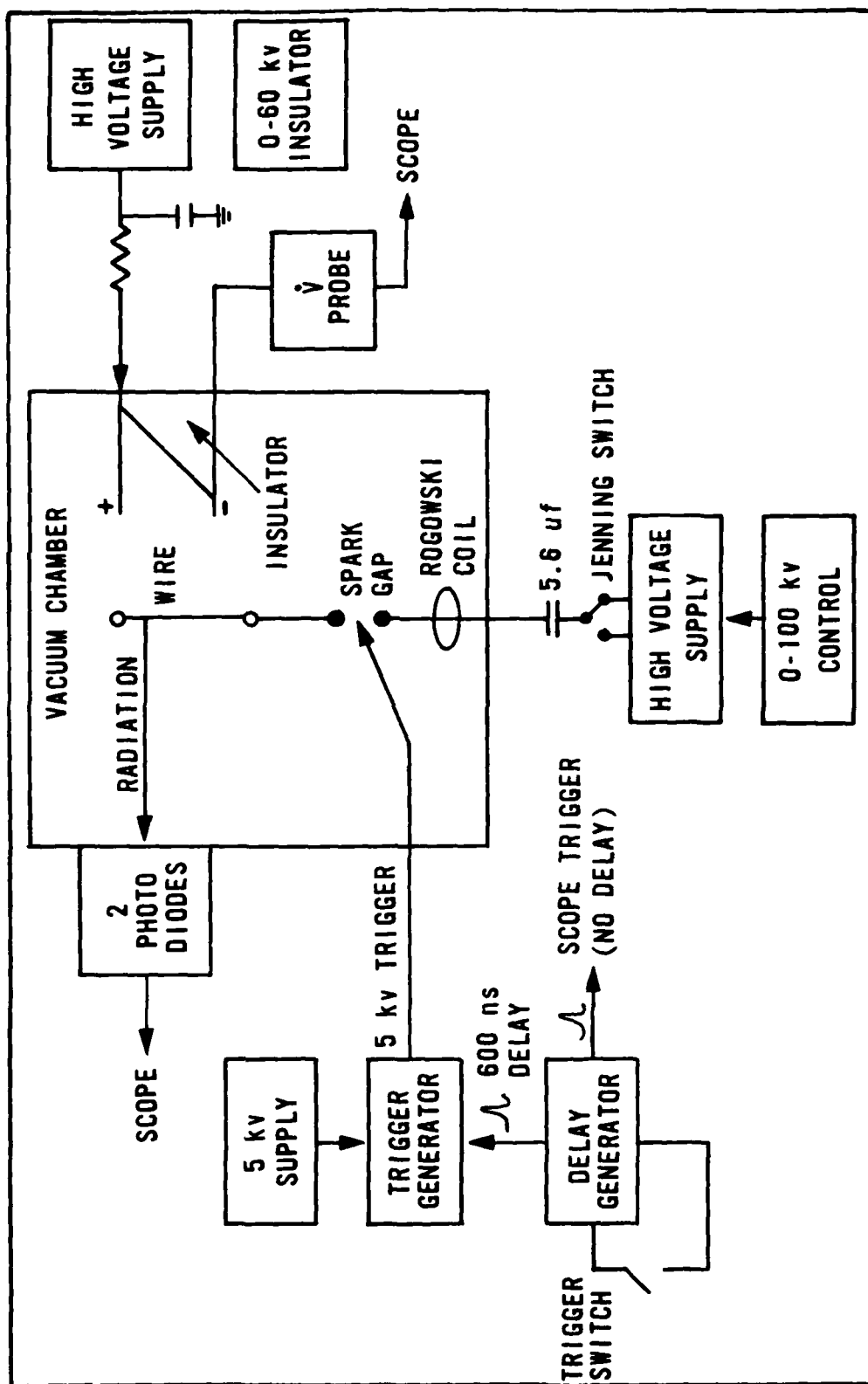


Figure 6. Vacuum Flashover Component Configuration

capacitor to ground through a resistor. The 0-60 Kv high voltage supply was used to provide a 20 Kv bias voltage across a pair of aluminum electrodes adjacent to the insulator under test. The electrodes were separated by a polyethylene insulator 1 cm thick and 3 cm long. The insulator was cut to form a  $45^{\circ}$  angle to the electric field between the electrodes.

With the capacitor charged and the insulator electrodes properly biased, a manual trigger switch was depressed to activate a delay generator. A trigger pulse was applied without delay to the oscilloscope trigger circuits to initiate the sweep prior to firing the system. After a 600 ns delay a trigger pulse was applied to a spiral trigger generator which provided a 20-30 Kv pulse to fire the spark gap.

Upon closure of the gap, the high current through the wire caused it to vaporize, ionize, and emit visible radiation. The radiation was measured by two photo diodes with narrow-band line filters. The photo diode outputs were used as the principle diagnostics to evaluate the approximate temperature of the radiator. The input to the photo diodes was selectively controlled by filters with about 100 Angstrom bandwidth centered at 706 nm and 423 nm. One filter was used for each diode. The diodes were placed approximately the same distance from the radiation source as the insulator to cause the impingent radiation intensity on both the insulator and the diodes to be nearly equal.

An analytic model was developed for evaluating the radiator temperature as a function of the output ratio of a given pair of detectors. The model was developed by relating the photo diode

response, and the filter transmission and bandpass to an assumed blackbody temperature (Ref 8). The data obtained were used to generate the curves in Figure 7. The approximate temperature of the radiating source was determined by computing the ratio of output signals of the photo diodes and applying the result to the appropriate curve. Figure 8 is a typical oscillograph of the diode outputs.

A one-mil tungsten wire was used as the radiator for most of the experiment. A few shots were made using one-mil aluminum, but little difference in radiator temperature was noted; therefore, since tungsten is more durable and easier to load in the vacuum chamber, it was chosen as the primary radiation source.

A  $dv/dt$  sensing probe was connected across the electrodes adjacent to the insulator and was used to determine whether or not the insulator flashed. If electrical breakdown occurred the instantaneous change in voltage across the insulator was sensed by the probe and was represented by an oscilloscope trace. Figure 9 is an oscillograph showing the occurrence of insulator flashover. Figure 10 is a scope trace in which the flashover did not occur. The upper trace in each figure is the 706 nm filtered diode output, and the lower trace is the  $dv/dt$  probe output signal. Figure 9 shows that the radiation produced by the exploding wire caused the insulator to flash almost instantaneously.

The plumbing between the source (wire) and the insulator was four inches in diameter and approximately eight inches long. To ensure that some mechanism other than radiation from the source was not causing the flashover, a plate was fabricated and placed inside the tube completely blocking the radiation path. Then, apertures



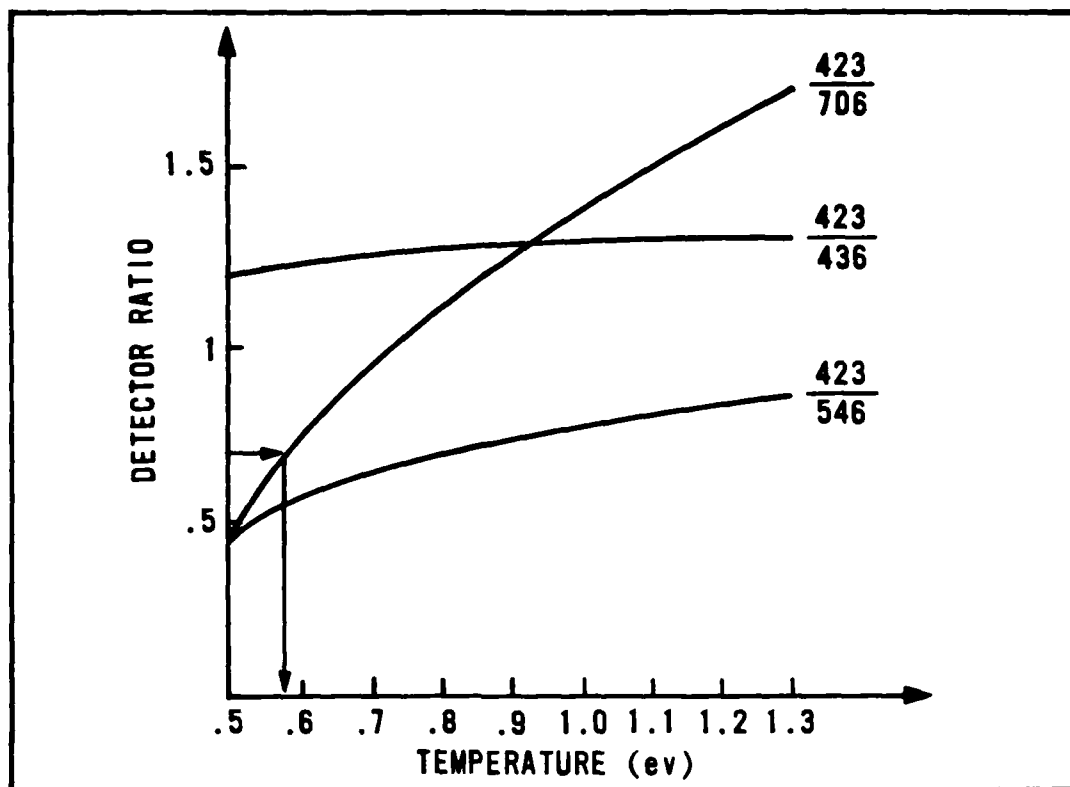


Figure 7. Radiation Temperature vs Detector Ratio

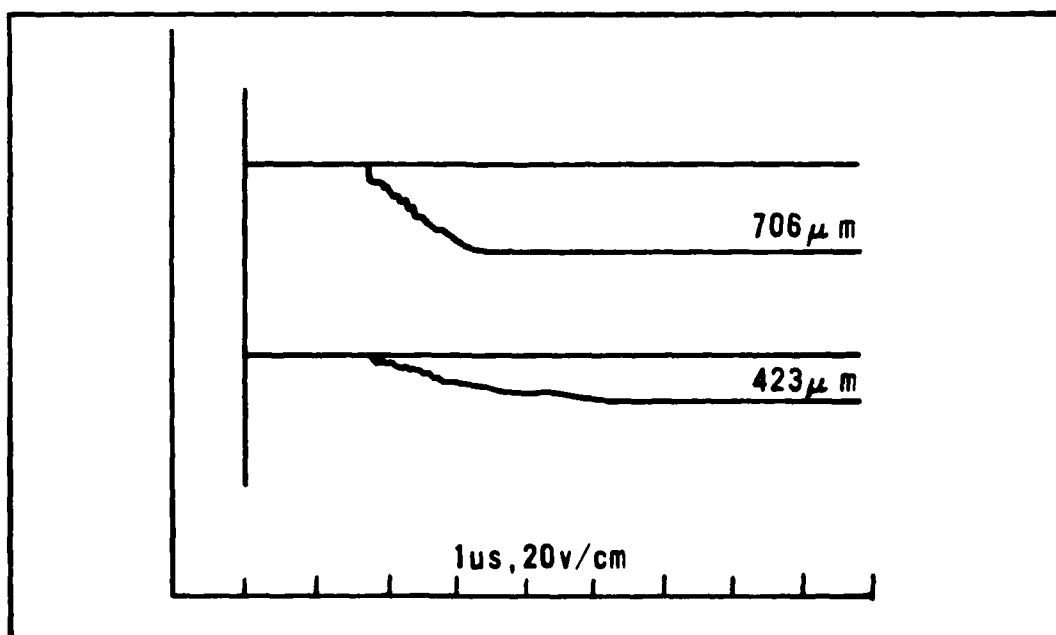


Figure 8. Photo Diode Output Traces

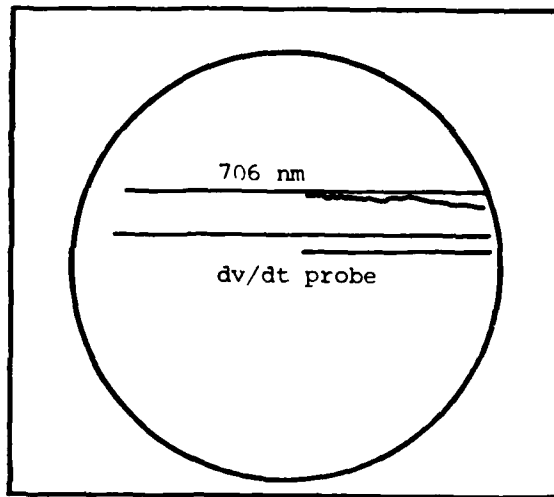


Figure 9. Oscilloscope Showing Insulator Flashover

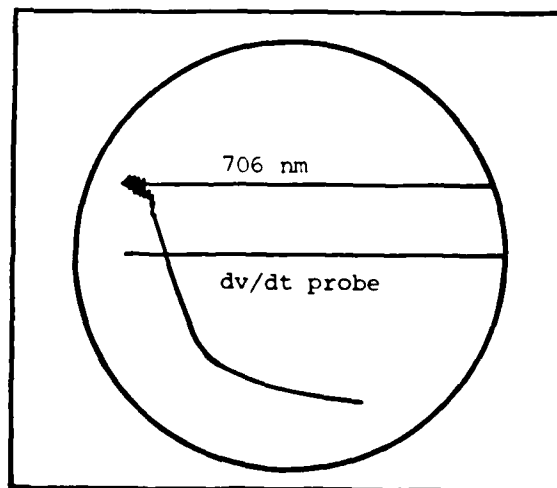


Figure 10. Oscilloscope Showing No Insulator Flashover

varying between 0.5 and 0.0156 inches were placed in the tube to vary the radiation intensity without changing the radiative spectrum. A quartz crystal was placed over the 0.5 inch aperture to determine the effect of a filter on the radiation. The findings from these variations are discussed in section IV.

#### Gap Closure

The gap closure experiment was performed using a 0.5 Megajoule inductive storage source. The source was made up of 48 capacitors of approximately 5.6 microfarads each, arranged in a series parallel configuration totaling 67.5 microfarads. The source was initially charged to 90 Kv, storing 273 Kilojoules of energy and then switched to the load through pressurized gas, railgap output switches. The energy was transported from the source through a transmission line and inductive store which had an inductance of 37 nanohenries. The transmission line consisted of two parallel conduction plates of aluminum separated by mylar insulation. The inductive store consisted of internal inductance of the system plus external inductance formed by increasing the separation of the line to several cm.

The energy in the capacitor bank was delivered to the experiment through an opening switch which was simply an exploding metal fuse. The fuse was made of aluminum foil and surrounded by sand (glass beads). The sand was used to quench aerosol products from the exploding fuse. The fuse length was 45 cm and was divided equally in two parallel sections to aid in assembly and improve quenching. When the bank was discharged, the fuse opened and delivered the energy stored in the inductance to a load through a closing switch.

The closing switch completed the circuit to deliver energy to the load. The self-breaking switch was constructed out of aluminum foil sandwiched between layers of polyethelene. The top polyethelene layer was perforated to a depth of 20 mils to promote multiple closing channels on the switch. Multi-channel breakdown provided lower inductance to the system which was desirable. Switch closure was self-initiated when the breakdown voltage was exceeded by the voltage produced by the current interrupting switch.

The energy delivered down the transmission line through the closing switch was applied to a modified SHIVA chamber, as shown in Figure 11. The chamber had ten 5.08 cm diameter ports to allow the placement of diagnostic equipment and two 15.24 cm by 5.08 cm windows to allow visual and photographic access to the load area. The machined aluminum chamber acted as an extension of the transmission line. Baffles were used to protect the insulator from flashover by making the path for radiation such that it would have to bounce off several surfaces before reaching the insulator. Breakdown in the vacuum gap was inhibited by the application of a clear acrylic coating to both chamber surfaces. The total voltage and current delivered to the load was 150 Kv and 0.6 Ma, respectively.

The load which produced the plasma consisted of an array of twelve 5 mil aluminum wires arranged in a circle 0.635 cm in diameter, and connected between two copper electrodes seperated by 2 cm. The circular arrangement was chosen to give symmetry to the source of radiation which was being generated. Aluminum wire was used to achieve the temperature range desired (1-10 ev). The copper electrodes used in the experiment are shown in post-shot configuration

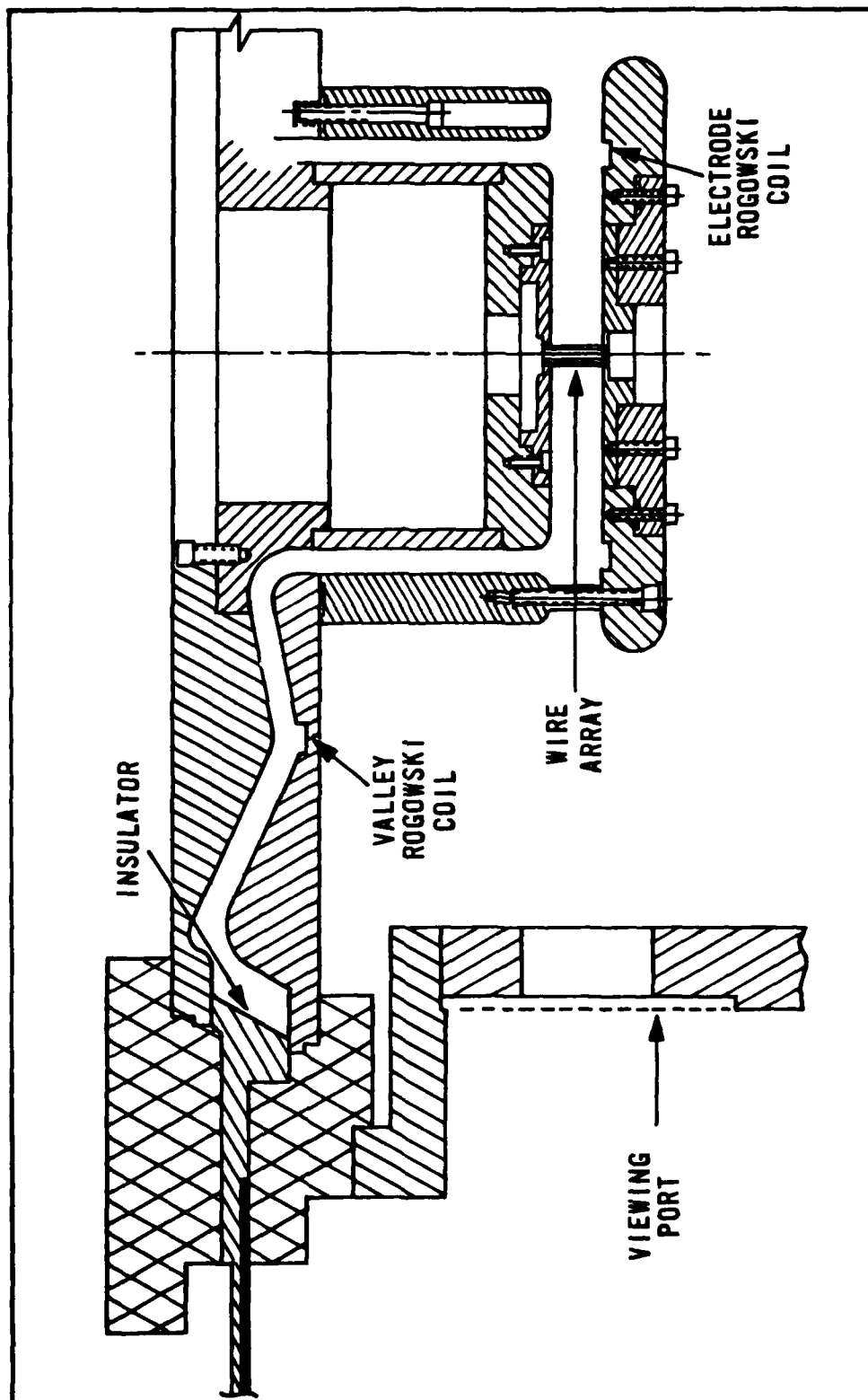


Figure 11. Modified SHIVA Chamber Cross-Section

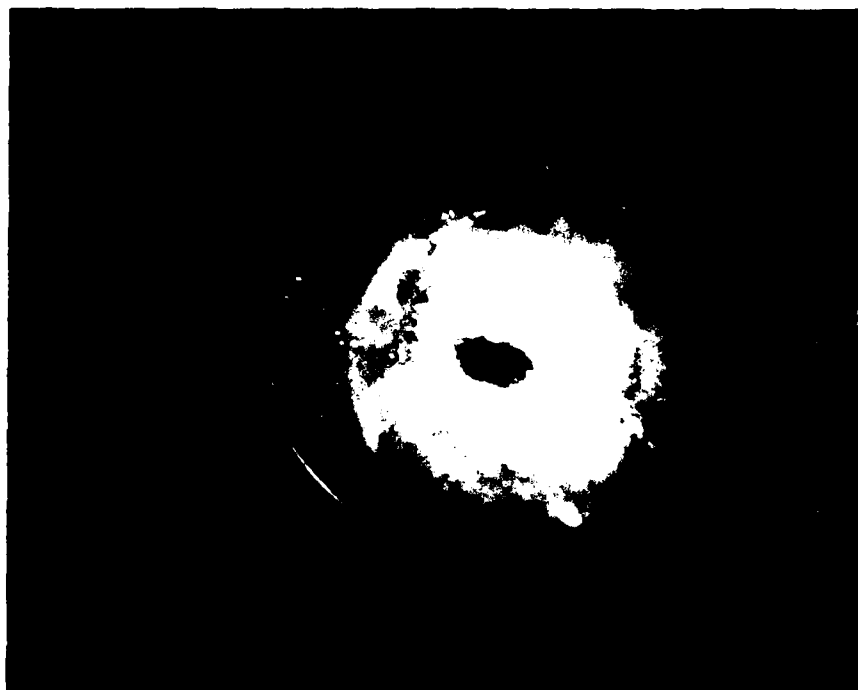


Figure 12A. Copper Anode, Data Shot



Figure 12B. Copper Cathode, Data Shot

in Figure 12. The indentation at the center of the electrodes was caused by z-pinching of the plasma as it collapsed under the driving force of the magnetic field of the discharge current.

#### Diagnostics

Diagnostics for the gap closure experiment were selected to determine temporal, spatial and spectral characteristics of the load and the motion of the electrode surfaces. Figure 13 shows the physical location of each diagnostic unit. The following diagnostics were used:

- a. Nitrogen lasers
- b. X-ray diodes
- c. Rogowski coils
- d.  $dv/dt$  probes
- e. Vacuum ultra-violet diodes
- f. Ultra-violet spectrograph
- g. Pinhole camera
- h. Streak camera
- i. Framing camera

System timing was accomplished with a delay trigger generator. The generator also provided a fiducial timing mark which was the timing reference. All signals were displayed on type RM 647 oscilloscopes. Oscilloscope traces were photographed using Poloroid type 410 film.

Four nitrogen lasers were used to provide backlighting for shadowgrams. Shadowgrams are used to record flow patterns and transient effects in detonation studies. The shadowgram system employed in the experiment imaged the event directly on a photographic

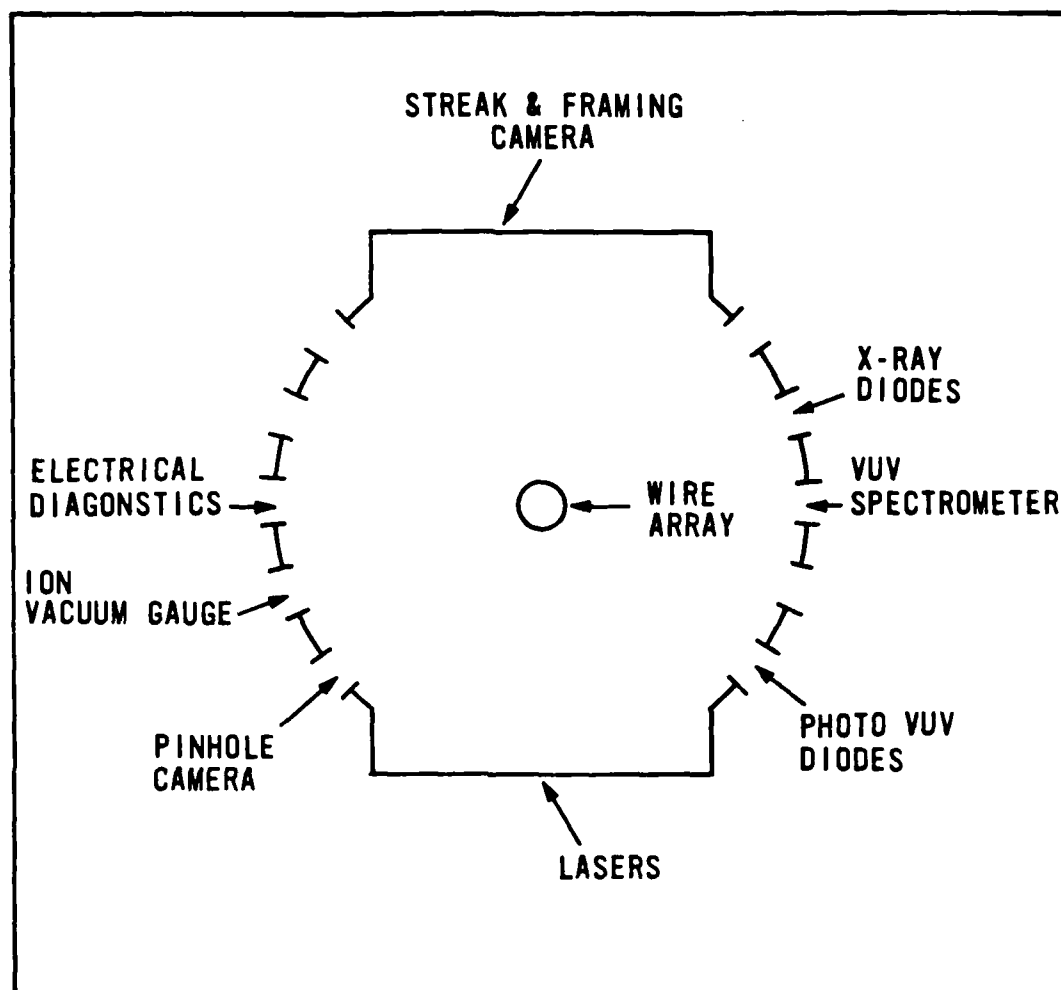


Figure 13. Vacuum Chamber Diagnostic Locations

plate by means of a field lens. When the lasers fired, the backlight produced caused exposure of the film. Developing reveals shadows caused by the flow pattern, etc. Intensity on the film varies as the second derivative of the plasma density along the beam path. Thus, the shadowgram is particularly appropriate for looking at situations with rapid changes in density, such as an advancing sheath.

The nitrogen lasers were supplied by the Los Alamos National Laboratory (LANL). The lasers provided a 10 nanosecond (FWHM) 2743 angstrom pulse and were aimed and fired in such a sequence as to



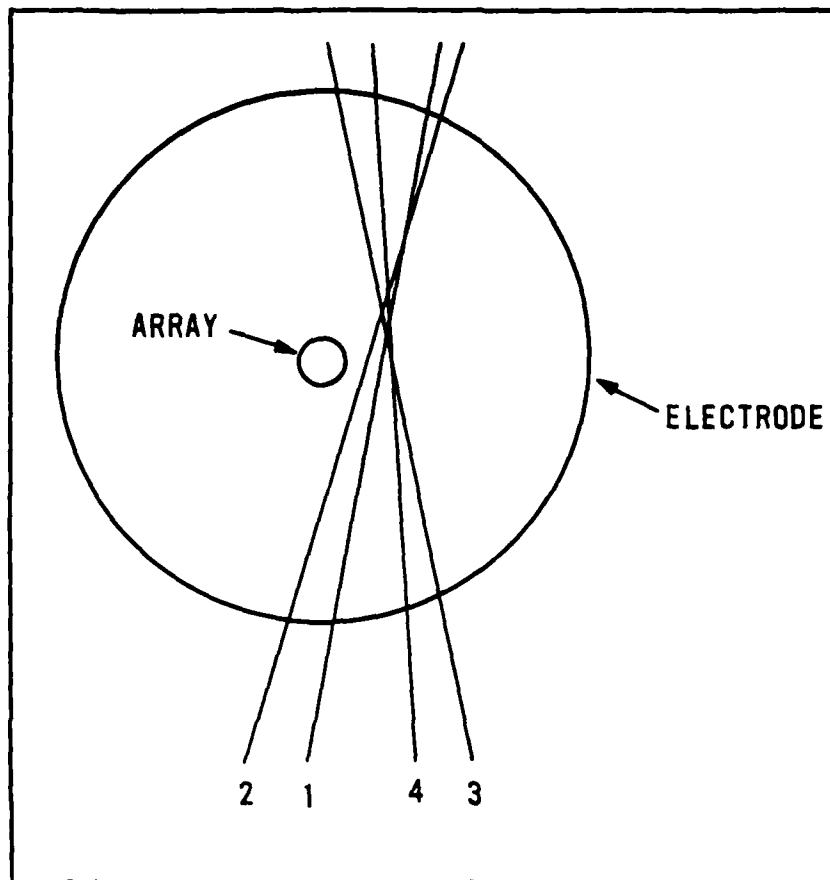


Figure 14. Nitrogen Laser Coverage

ensure complete coverage of the area adjacent to the wire array. The laser coverage is shown in Figure 14. The nitrogen beam entered the test chamber through a 15.24 x 5.08 cm quartz window. Since the target was a wire array with good visibility between the wires, the lasers could be aligned at any time without removal of the array. A pre-shot photo, shown in Figure 15, was taken showing the wire array as well as both electrode surfaces. The film was type 55 Poloroid which provided both positive and negative photos. The pre-shot photo was used as a reference and compared with a data photo, as shown in Figure 16. The pre-shot and post-shot photos were both enlarged to the same size. Then, the dimensions of the gap from the pre-shot

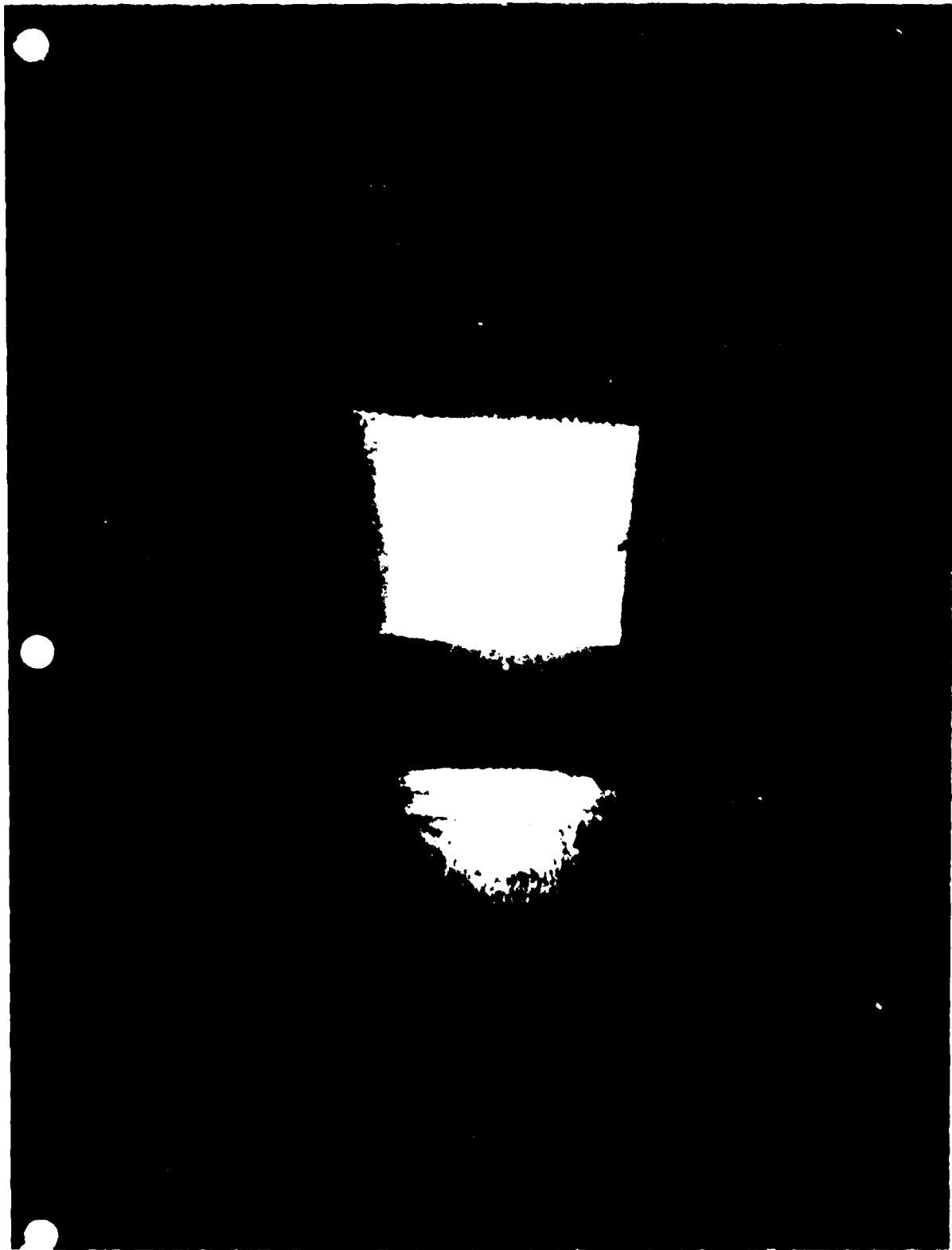


Figure 15. Laser Shadowgram, Pre-Shot

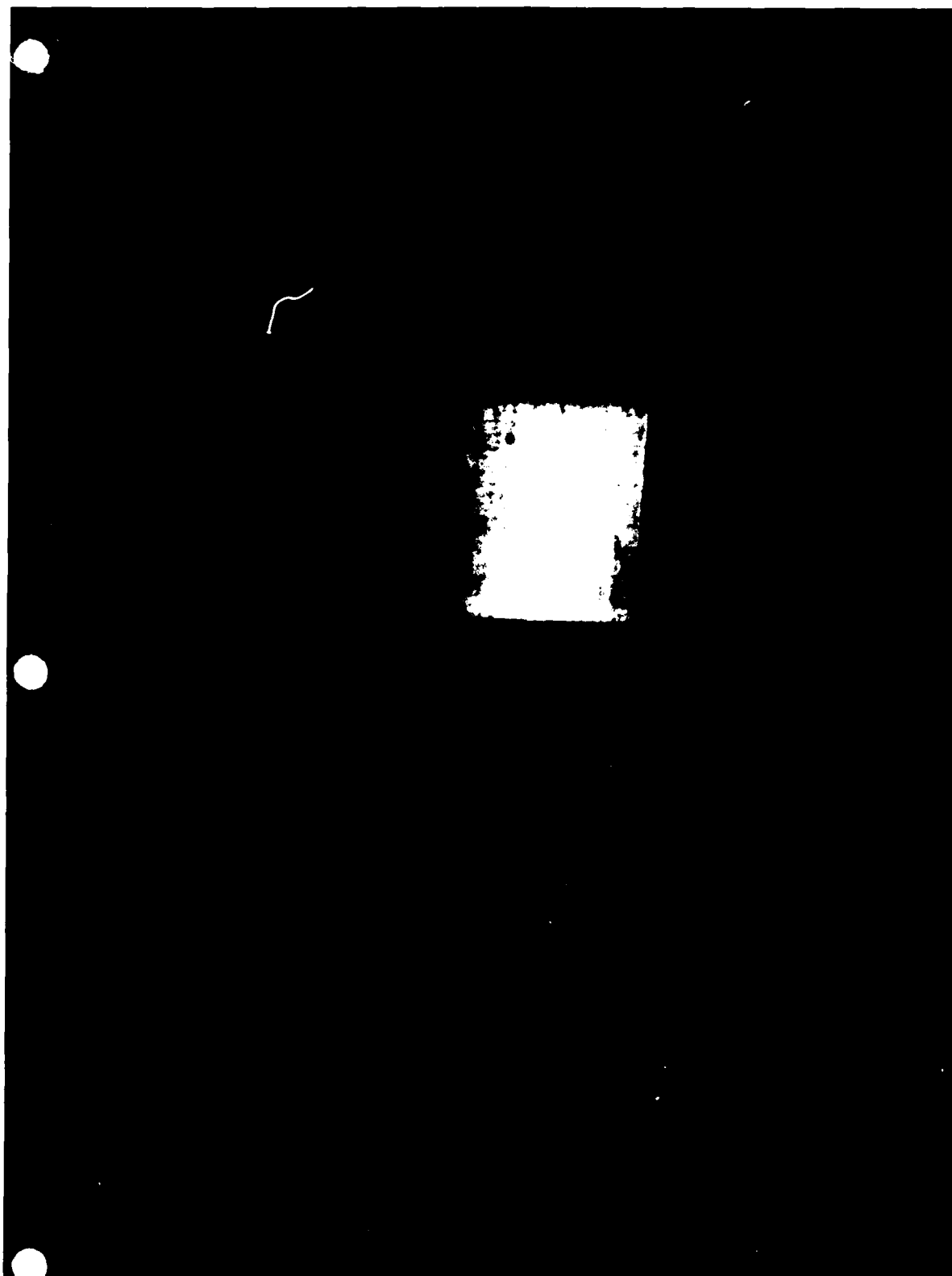


Figure 16. Laser Shadowgram, Data Shot

photos were compared with those of the post-shot photos. The gap closure rate was determined by subtracting the post-shot gap measurement from that of the pre-shot. Fiber optic cables connected between the lasers and an oscilloscope were used to determine when the lasers fired. The oscillograph was recorded on film for later data reduction. The gap closure rate was determined using relative timing data and shadowgraphs showing the position of the ablation in the gap.

X-ray photo diodes were used to obtain a temperature profile of the exploding wire array. Figure 17 is a drawing of the X-ray diode cross-section. Figure 18 shows the electrical connection of the diodes. X-ray photo diodes were used because of their rapid response to sub-microsecond radiation. This allowed a measurement before hot gasses and debris from the exploding wire array could destroy the detectors. Filters and flux screens were used with the photodiodes, and only these had to be replaced after each shot. Filter composition and photo cathode material determined spectral response of the detector and flux screening using electro-etched nickel screen of known transmission adjusted detector sensitivity to prevent space charge saturation of the diodes. An array of four X-ray photodiodes was used to allow coverage of a broad spectrum of temperatures. Table I gives the material used for the anode filter combination as well as the attenuation required and temperature ranges. The transmittance of the 2000 line screen was 0.22 and that of the 100 line screen was 0.82.

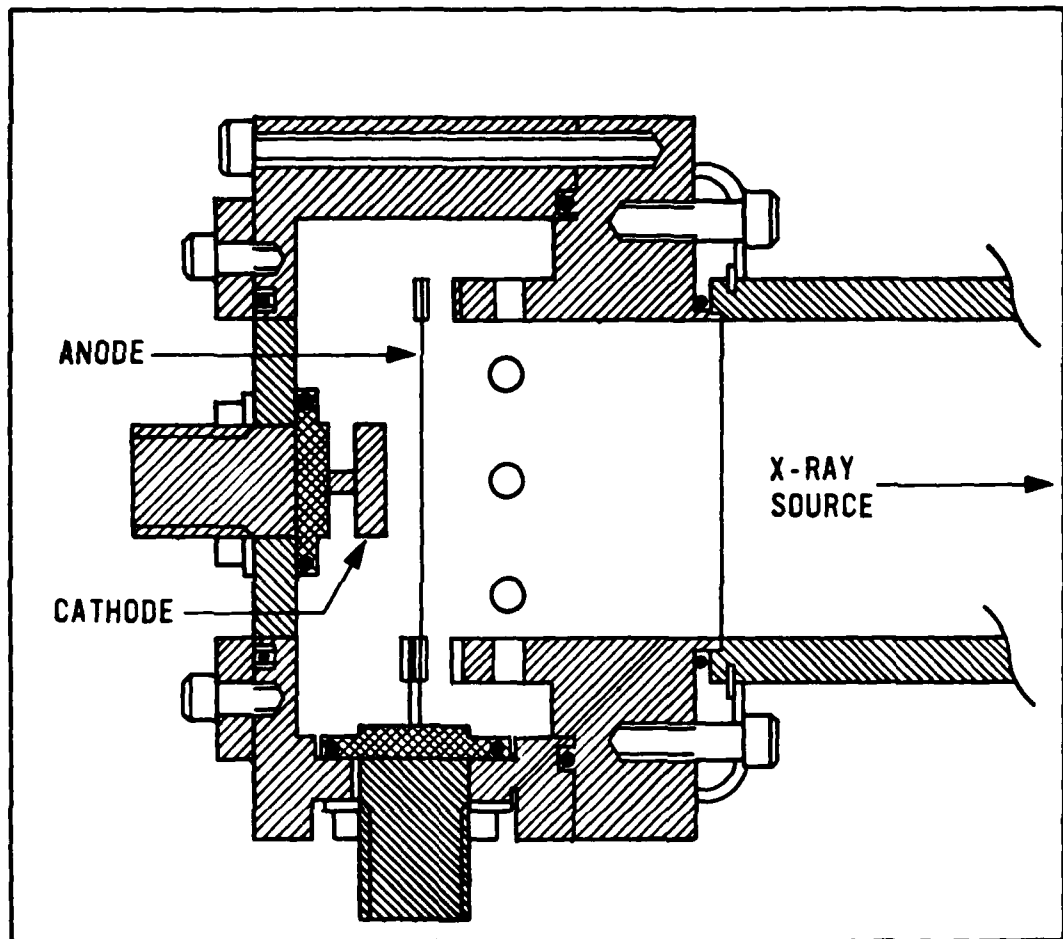


Figure 17. X-ray Diode Cross-Section

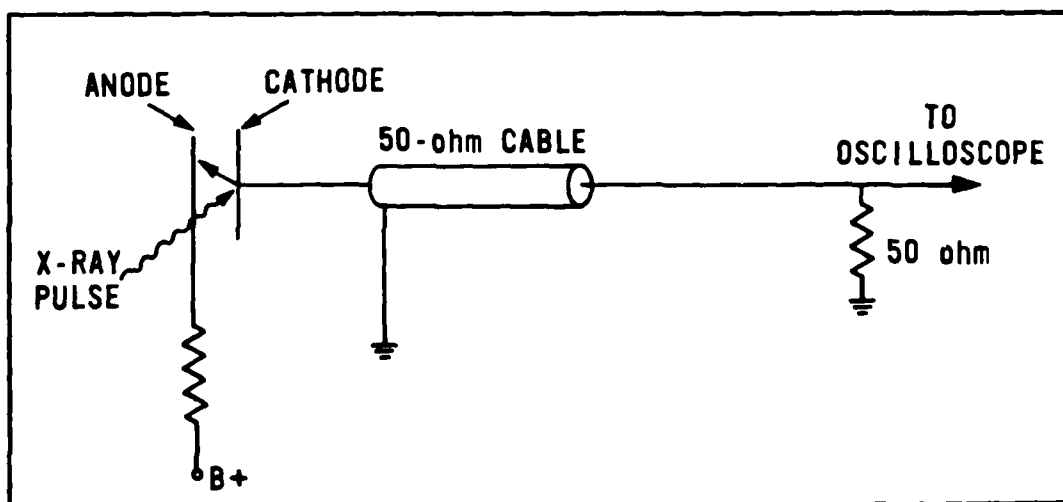


Figure 18. X-ray Diode Circuit Configuration

Table I

Electrode Material	Attenuation (lines/inch)	Sensitivity (amp/megawatt)	Temperature Range (ev)
Al/bare	3@ 2000	4000	10-40
Al/Al	2@ 2000	114	15-73
Al/2Al	100	40	25-73
Al/Formvar	100	42	70-200

Rogowski coils were used to obtain current measurements. It was essential to know how much current was delivered to the load. Coils were located at various positions in the chamber to obtain as much information as possible. The location of the Rogowski coils is shown on the line drawing in Figure 11. The bank coil was used to determine what current was delivered by the bank. Two coils were mounted on the outside of the chamber. One was wrapped clockwise and the other was wrapped counter-clockwise. This configuration was used to eliminate electrical coupling. A coil was placed just inside the vacuum chamber near the dielectric-vacuum interface to insure that the current had progressed across the the interface without any losses. This coil seemed to present a problem on the first few shots. It had a tendency to cause arcing in the chamber and prevented complete transfer of energy to the load. The coil was replaced by a valley coil. Changing the position of the coil eliminated the arcing problem and still allowed monitoring of the current from the dielectric-vacuum interface. A final Rogowski coil was located on the electrode plate. It was used to determine the exact current delivered to the load. A typical trace of a Rogowski coil is shown in Figure 19. Integrators and attenuators were used to obtain these traces.

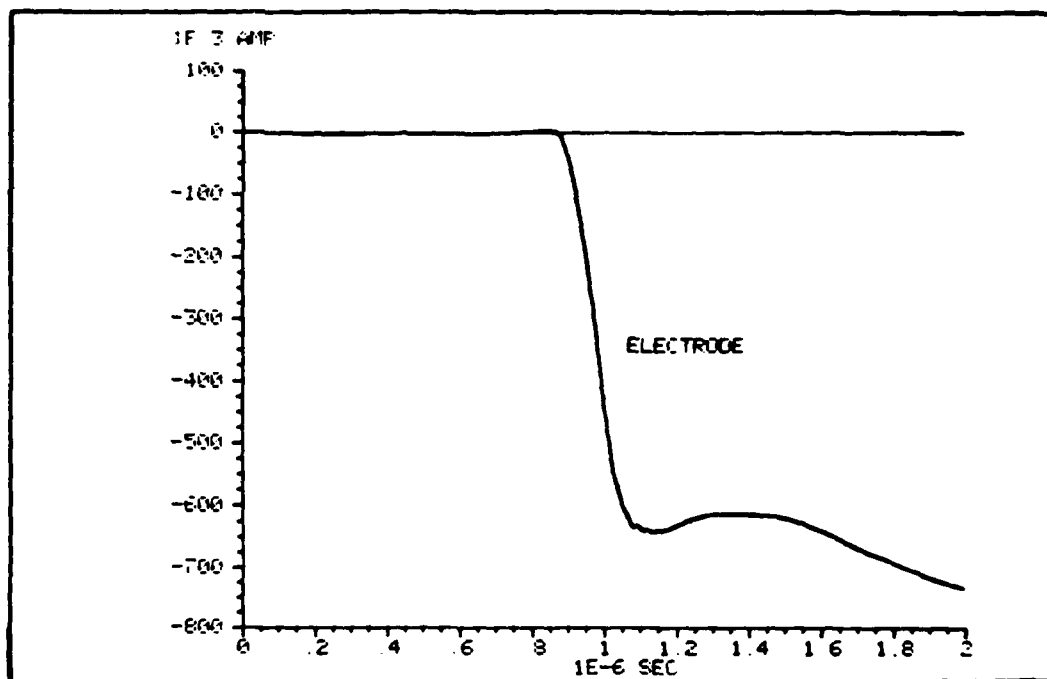


Figure 19. Typical Rogowski Coil Signal

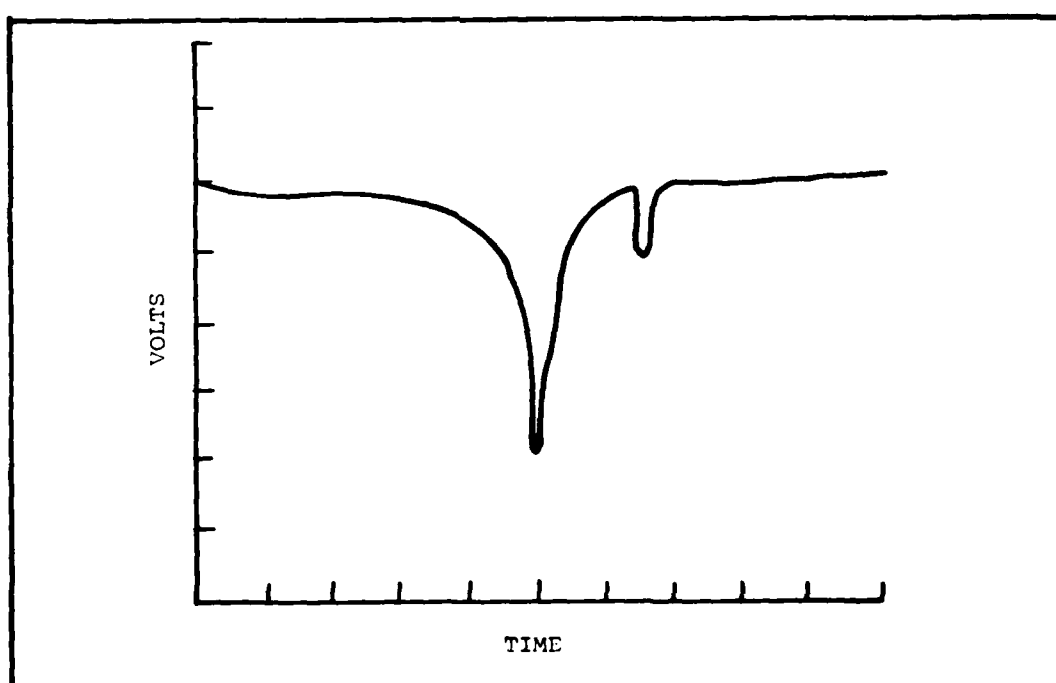


Figure 20. Typical  $dv/dt$  Probe Signal

Voltage levels were determined using two  $dv/dt$  probes. One probe was located on the bank and the other on the chamber side of the output switch. These were used to monitor the operation of the bank, store, and switching system. A typical oscillograph from a  $dv/dt$  probe is shown in Figure 20. The large negative spike occurs when the bank fires. The small spike is the fiducial reference marker.

A pinhole camera was used to determine if any hard X-rays were being produced during the explosion and subsequent pinching of the plasma. Various combinations of filters, attenuators, and pinhole sizes were used with limited success. The major problem with pinhole cameras was their sensitivity to visible light. Also, during alignment of the streak and framing cameras, the pinhole camera may have been exposed because of the need for a high intensity light. This problem could not have been corrected by waiting until the other cameras were aligned because the pinhole camera was one of the first pieces of diagnostic equipment installed on the test chamber.

Optical streak and framing cameras were used to obtain data from the exploding array. The streak camera was expected to supply gap closure and plasma radius data as a function of time. The framing camera was to supply gap closure versus time data. High speed photographic measurements were only marginally successful because of triggering problems. The cameras either triggered prematurely or not at all when the inductive storage bank was fired. However, they worked properly before and after each shot. The problem was finally overcome by using optical triggering.

A one-half meter vacuum ultraviolet spectrograph was employed to



obtain a spatially resolved but time integrated spectrum. The aperture for the spectrograph was a 100 micron entrance slit. A curved grating of 600 lines per inch was used to obtain a spectral range between 35 and 750 Angstroms. Kodak 101-01 film produced an approximate resolution of 5 angstroms. A blackbody temperature of 10 ev was determined to be the characteristic temperature of the exploding array. The dominant spectral line was the Al IV ion.

#### IV. Results

The results of the insulator flashover and gap closure experiments are presented separately in this section. Insulator flashover influenced by different parameters are described. The gap closure rate determined from shadowgrams is given. Gap closure, power, radiative energy, and temperature are also discussed.

##### Insulator Flashover

Initially, the experiment was configured to allow radiation emitted by the wire source to travel unimpeded to the insulator. In this case the insulator flashed virtually instantaneously. The radiation path was then completely blocked by a metal plate to ensure that some mechanism other than photon energy was not causing surface flashover. Numerous shots were fired, and the insulator never flashed.

When apertures were used the insulator flashed, irrespective of the aperture diameter. A clear quartz window was placed over the largest aperture used, and in several shots no flashover occurred. Although smaller apertures were not tested, it is reasonable to assume that the result would be the same with the quartz window in place.

The temperature of the radiator was measured for every shot whether flashover occurred or not. The temperature in every case was approximately 0.5 ev. It would seem that one should expect some variation in temperature, particularly when the radiator was changed from tungsten to aluminum. Thus, other combinations of photo diodes were tried, and the initial result was verified in each case.

### Gap Closure

Useful data was obtained from the ultra-violet spectrograph, Rogowski coils,  $dv/dt$  probes, streak camera and laser shadowgraphs. Data from this instrumentation was used in determining the temperature of the plasma as well as the gap closure rate. The experiment was conducted using a vacuum of  $1 \times 10^{-6}$  torr or better.

The voltage measurement at the chamber input was 150 Kv and the current through the electrodes was 600 Ka. The approximate inductance of the chamber was 10 nanohenries.  $di/dt$  through the electrodes was  $5 \times 10^{12}$  amps per second. These values indicate that a 50 Kv ( $L di/dt$ ) drop occurs between the insulator and the electrode. Thus, the voltage at the electrode may be crudely estimated at 100 Kv. The approximate values of voltage and current at the electrode provide  $6 \times 10^{10}$  watts of electric power delivered to the plasma and the magnetic field in the immediate vicinity of the plasma.

Throughout the test the vacuum gap was closing at points other than at the electrodes. When this happened loss of energy occurred and short circuited the energy before it reached the load. Major problem areas were at the triple junction of the insulator, electrode, and vacuum and in some of the valleys of the test chamber. If both chamber surfaces were coated with a thin coat of Krylon clear acrylic paint, chamber breakdown could be postponed until after the time of interest; however, this presented a new problem in that the test chamber had to be sand blasted and cleaned before the experiment could be continued to prevent closure in portions of the vacuum feed beyond the view of the diagnostics. A Krylon coating smoothed out the

irregularities in the chamber surface and reduced the electric field enhancement at microprotrusions.

Streak camera photographs and results from the ultra-violet spectrograph were used to determine the temperature of the load. The streak camera photo in Figure 21 shows a dark center and an optically thin outer edge. The outer edge needs to be treated as a line radiator. Using this idea and the data from the spectrograph, an equivalent blackbody and line radiator temperature was determined. From the spectrograph it was determined that Aluminum IV ions were the most prevalent ions present. A temperature of 11-16 ev will give high concentrations of Aluminum IV ions. The power radiated from an 11 ev plasma was calculated to be  $6 \times 10^9$  watts as compared to  $6 \times 10^{10}$  watts of electrical power input. This is equivalent to six kilojoules of energy.

The current flowing through the plasma caused an azimuthal magnetic field which pinched the plasma column, causing a rapid increase in pressure which produced a deformation in the electrode center. This deformation was approximately one centimeter deep and three centimeters in diameter. The damage was repaired by pressing the electrode from the opposite side to flatten the surface.

Radiated energy from the plasma causes a rapid boiling or vaporization of the electrode surface. As the vaporized copper boils off, the ablative electrode surface moves across the gap. This movement of ionized gas was photographed using nitrogen lasers as a bright light source for shadowgrams. By using the first indication of current flow in the electrode as a time reference and measuring the distance that the ablative surface traveled, a percentage of gap

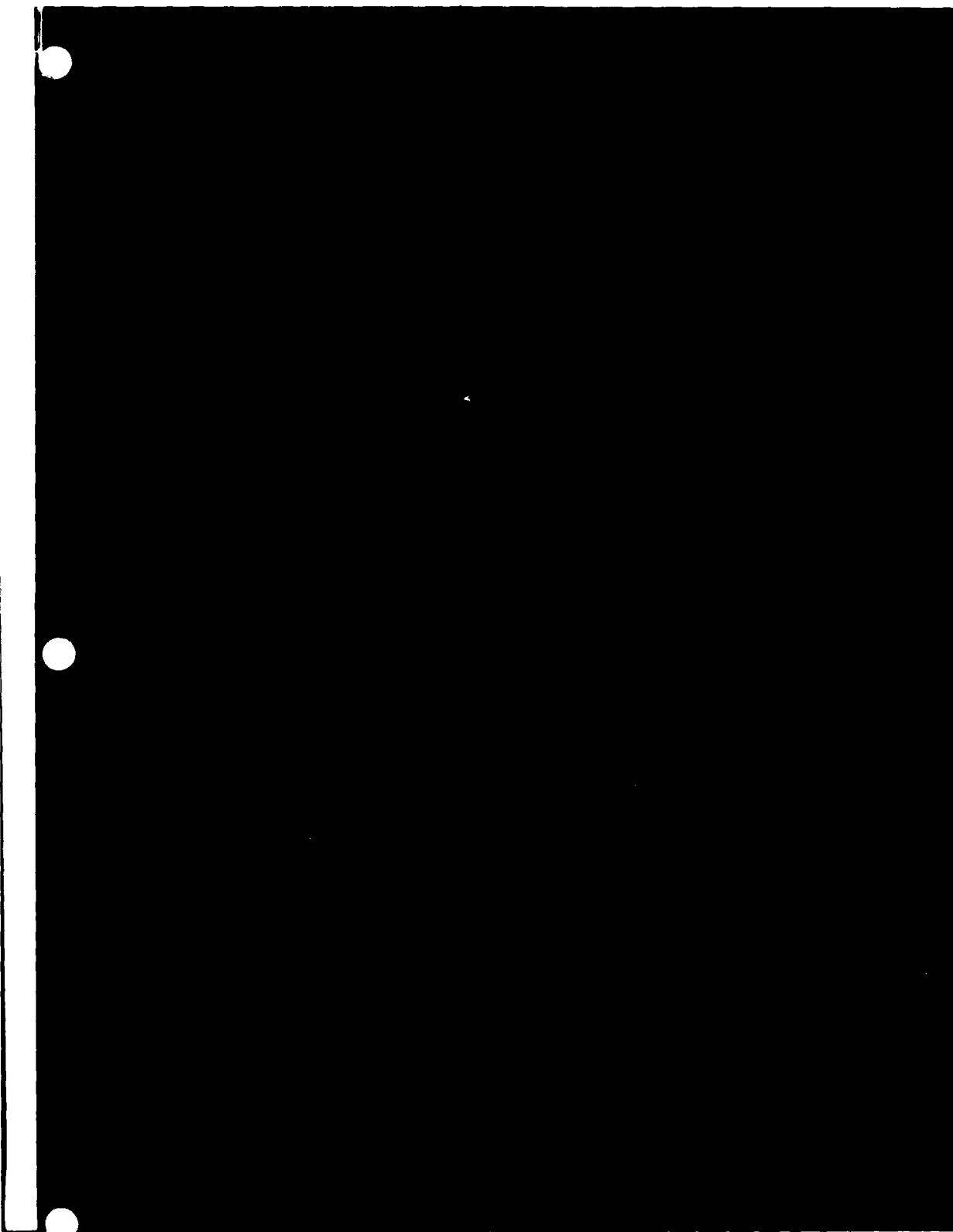


Figure 21. Streak Camera Photo

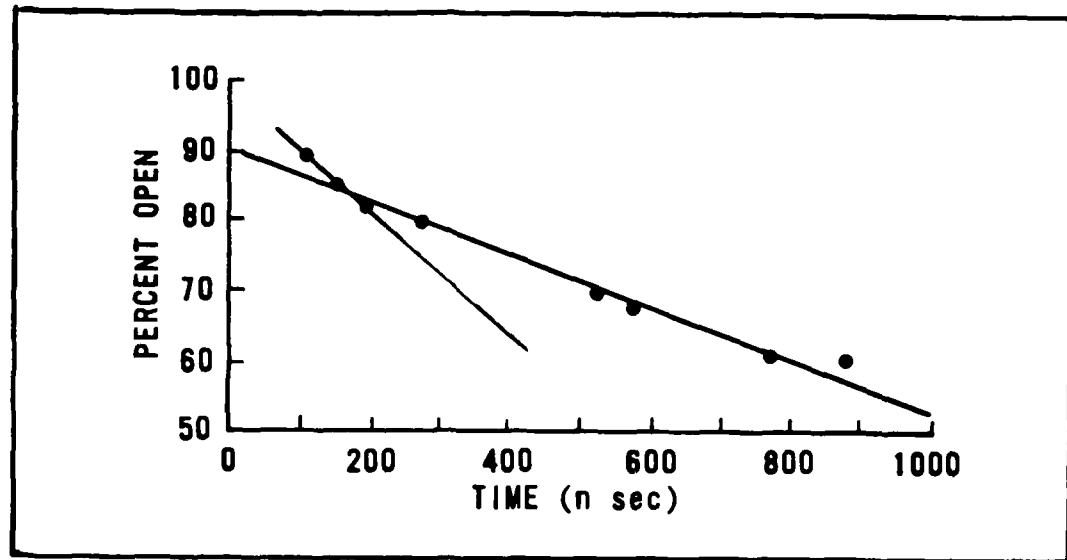


Figure 22. Percentage of Gap Closure

closure was calculated as a function of time. Closure percentages are plotted in Figure 22. As shown in Figure 19 the current rose to a peak in 200 nanoseconds. Figure 22 shows that for the first 200 nsec the gap closes at a rate of 2 cm/usec (one centimeter from each side). After 200 nsec the closure rate slows to .35 cm/usec during which time the current, and hence, the magnetic field remains nearly constant.

## V. Discussions and Conclusions

In this section conclusions drawn from the results in Section IV are given. The effect of a quartz window on short wavelength radiation is discussed. The Maxwell Laboratory gap closure experiment is contrasted with the current effort and reasons are given for differences between the two. Finally, a value for the velocity of the ablated surface is given.

### Insulator Flashover

Figure 23 is a blackbody curve for a typical radiator. At some wavelength the maximum power density of the radiator is reached, and then, the average power density of the radiator decreases proportionately with the wavelength of the emitted radiation. At very short wavelengths, line radiation may occur at powers well in excess of that radiated by the blackbody (appearing as spikes in the figure) and which may be sufficient to initiate the immediate breakdown of the insulator.

Figure 24 is a transmittance curve for the quartz window used in the experiment. The window becomes nearly opaque to photon energy below about 1600 Angstroms. Recall that the threshold for ionization of the polyethylene insulator was calculated to be about 1240 Angstroms. Thus, at short wavelengths with the window in place, insufficient energy is getting to the insulator to initiate an avalanche breakdown.

Without the use of a quartz window to filter incident radiation, the insulator flashover could not be controlled. With the window in

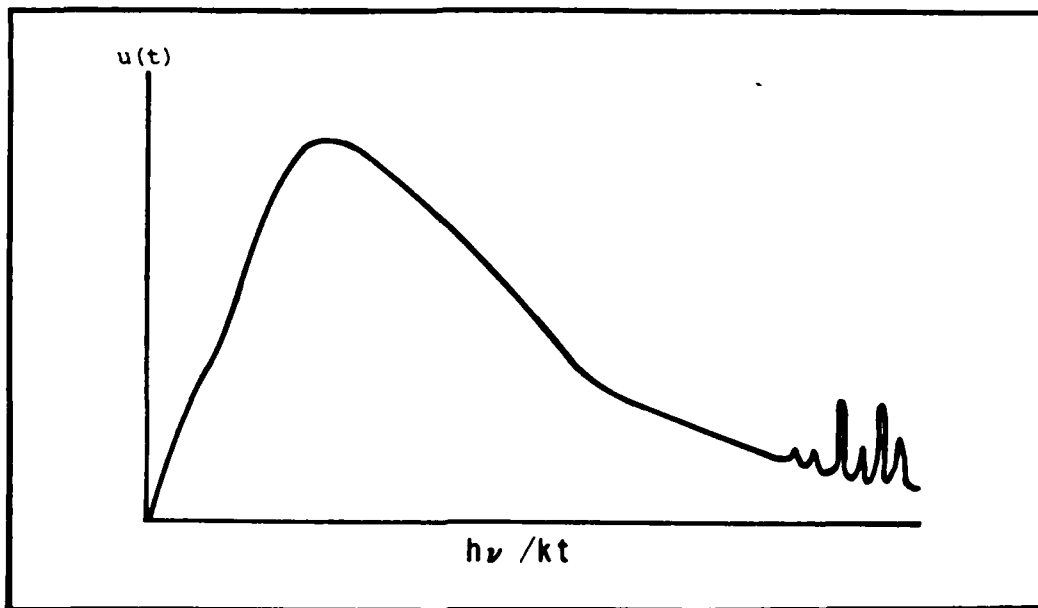


Figure 23. Blackbody Curve With Line Spectra

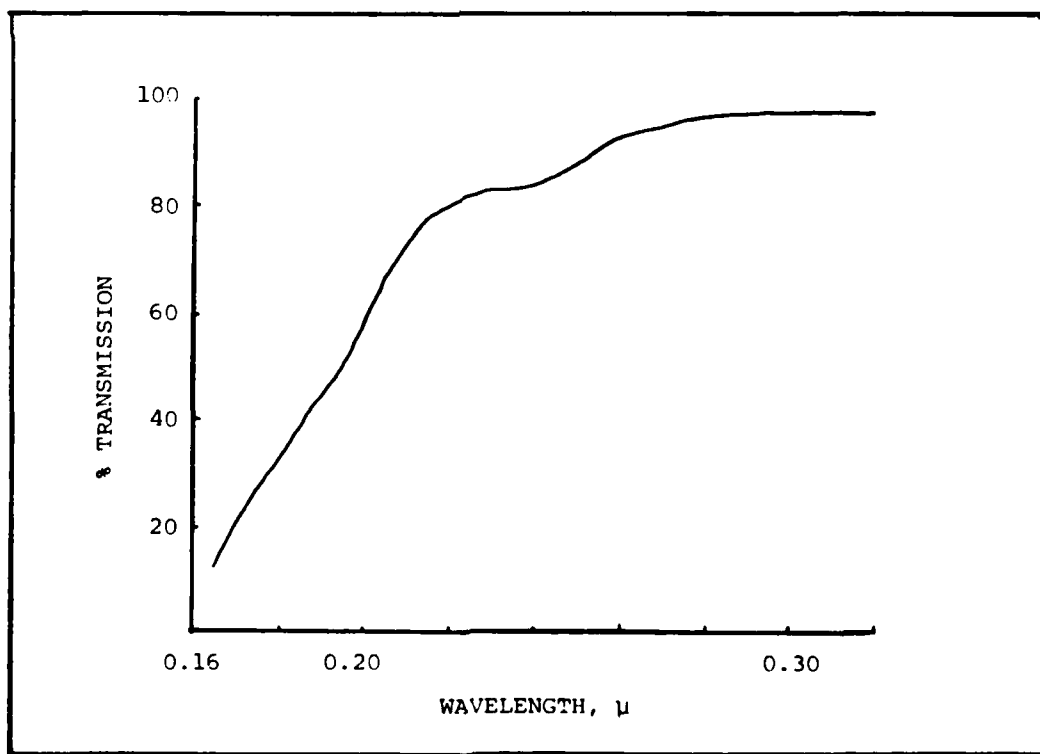


Figure 24. Quartz Window Transmittance



place, electrical breakdown across the insulator never occurred. Apparently then, there is some threshold at which the insulator will flash and below which the large amounts of power may be deposited at the surface without inducing breakdown.

#### Gap Closure

A value for the velocity of the ablated surface was calculated and found to be 0.35 centimeters/microsecond. This value is an order of magnitude smaller than that observed by Maxwell Laboratory (Ref 6:3-3). The temperature of the plasma used by Maxwell appears to be approximately the same magnitude as that used in this experiment.

These results do not compare with those found by Maxwell Laboratory. Two major differences exist between the two experiments. First, the current in this experiment rose to 600 Ka and remained at that level during the period of interest. This steady current produced a uniform magnetic field in the gap which suppressed the expansion of the ablated surface. In the Maxwell experiment the current rose to 600 Ka and then fell off rapidly (Ref 6:2-4). The decrease in current reduced the magnetic field being generated and allowed the ablative surface to expand at a higher velocity. The second difference was the source of light for the shadowgrams. A nitrogen laser at a wavelength of 2743 Angstroms was used as a source of light in this experiment. A ruby laser at a wavelength of 6943 Angstroms was used in the Maxwell experiment. The different laser wavelengths would produce characteristically different fringe patterns on the shadowgrams.

The ultra-violet laser measurement might also be expected to

suggest slower advance of the ablative front on critical density grounds alone. Since the maximum density that light can penetrate goes as  $1/\lambda^2$ , the 2.5 times shorter wavelength nitrogen light would be expected to penetrate a plasma having six times the density of that penetrated by ruby light. Thus, the ablative "front" would be at higher density or nearer the electrodes.

## VI. Recommendations

Based on the results and conclusions described previously, recommendations for future work are given. Many additional studies could be initiated as a result of the experiments described in this report. Only work which is important in the near term for SHIVA applications is discussed.

### Insulator Flashover

The fact that the insulator in this experiment flashed regardless of aperture size with no filter and never flashed when a quartz window blocked the radiation path is insufficient to allow one to conclude that this is a means of preventing insulator flashover in vacuum power equipment. Additional experiments are required to verify the inhibitive quality of quartz or comparable materials. However, it must be remembered that quartz itself is a dielectric material and, at some voltage, will be subject to flashover; thus, there is a practical limit to the utility of such materials as radiation filters in power flow.

To decrease the effect of the dielectric limitation noted above, experiments might be conducted to determine an effective means of reducing or eliminating high energy photons without the use of filters. Some success has already been attained in SHIVA experiments by using a baffled feed to the load, as described earlier in this report. This configuration, however, has not eliminated the flashover problem and additional improvements are required.

### Gap Closure

Additional experiments should be conducted to determine if the gap closure rates are dependent on electrode material. Once the gap closure rates have been determined for various electrode materials, testing should be conducted to determine if the gap closure rate can be effectively retarded.

Since Krylon acrylic paint appears to retard conductor flashover an attempt should be made to determine if patching of the acrylic surface is feasible. This would reduce the amount of time needed to resurface the chamber.

### Bibliography

1. Reinovsky, Robert, Air Force Weapons Laboratory Letter Proposed Thesis Topics, March 1981.
2. Bergeron, K. "Theory of the Secondary Electron Avalanche at Electrically Stressed Insulator-Vacuum Interface," Journal of Applied Physics, 48 (7): 3073-76 (July 1977).
3. Milton, O. "Pulsed Flashover of Insulators in Vacuum," IEEE Transactions on Electrical Insulation, EI-7 (1):9-15 (March 1972).
4. Gleichauf, Paul H. "Electrical Breakdown over Insulators in High Vacuum," Journal of Applied Physics, 22 (5):35-541 (May 1951).
5. Gleichauf, Paul H. "Electrical Breakdown over Insulators in High Vacuum," Journal of Applied Physics, 22 (6):766-771 (June 1951).
6. Brannon, J. et al, Final Report Vacuum Transmission Line Technology, Maxwell Laboratories, Inc. Report MLR-1050 submitted to AFWL/NTYP, Kirtland AFB, New Mexico 87117, (Jan 1981).
7. Reinovsky, Robert E. et al, "Soft X-Ray Effects on Vacuum Power Transport," unpublished paper, Air Force Weapons Laboratory, Advanced Concepts Branch, Kirtland Air Force Base, New Mexico 87117, (Jan 1981).
8. Degnan, J. Laboratory Notebook and Computer program for Modeling Radiator Temperature, Air Force Weapons Laboratory, Advanced Concepts Branch, Kirtland Air Force Base, New Mexico 87117.
9. De Turreil, C. H. and Shivastava, K. D. "Mechanism of Surface Charging of High-Voltage Insulators in Vacuum," IEEE Transactions on Electrical Insulation, EI-8 (1):17-21 (March 1973).

### Vita

Richard Blaher was born 27 February 1946 in Wausau, Wisconsin. He grew up in Pueblo, Colorado where he graduated from South High School in 1964, and enlisted in the United States Air Force. After serving seven years as an airborne navigation equipment repairman he attended Colorado State University under the Airman Education and Commissioning Program. He received a Bachelor of Science Degree in Electrical Engineering in 1975. He was then assigned to the Rome Air Development Center at Griffiss Air Force Base, New York, where he worked as an infrared system design engineer in the cruise missile Automatic Terminal Homing Program. He received a Master of Science Degree in Management Science from the State University of New York, Binghamton, in 1980. Currently he is assigned to the School of Engineering, Air Force Institute of Technology, Wright-Patterson Air Force Base, Ohio. He is a member of Eta Kappa Nu.

Permanent Address: 6422 Concordia Rd., N.E.

Albuquerque, New Mexico 87111

### Vita

Oakley Mitchell was born 26 November 1947 in Saginaw, Michigan. He graduated from Arthur Hill High School in 1965 and attended Delta College in Saginaw for two years before enlisting in the United States Air Force. After serving six years as a Missile Instrumentation Technician at Holloman AFB, New Mexico, he was selected to attend New Mexico State University in the Airman Education and Commissioning Program. He received a Bachelor of Science Degree in Electrical Engineering in 1974. He was commissioned a second lieutenant after graduation from Officer Training School in 1974. He was assigned to Hanscom AFB, Massachusetts as a Radar Test Engineer with the Airborne Warning and Control System (AWACS) Program Office. In 1977 he was transferred to Tinker AFB, Oklahoma where he served as the site manager of the AWACS program. He received a Master of Business Administration Degree from Oklahoma City University in 1979 and entered the School of Engineering, Air Force Institute of Technology, in June 1980. He is a member of Eta Kappa Nu and Blue Key.

Permanent address: 8500 Monitor NE

Albuquerque, New Mexico 87109

UNCLASSIFIED

SECURITY CLASSIFICATION OF THIS PAGE (When Data Entered)

REPORT DOCUMENTATION PAGE		READ INSTRUCTIONS BEFORE COMPLETING FORM
1. REPORT NUMBER AFIT/GA/EE/81D-12	2. GOVT ACCESSION NO. AD-A15516	3. RECIPIENT'S CATALOG NUMBER
4. TITLE (and Subtitle) SOFT PHOTON EFFECTS ON VACUUM POWER FLOW		5. TYPE OF REPORT & PERIOD COVERED MS Thesis
		6. PERFORMING ORG. REPORT NUMBER
7. AUTHOR(s) Richard J. Blaher    Oakley J. Mitchell Capt                    USAF                    Capt                    USAF		8. CONTRACT OR GRANT NUMBER(s)
9. PERFORMING ORGANIZATION NAME AND ADDRESS Air Force Institute of Technology (AFIT-EN) Wright-Patterson AFB, Ohio 45433		10. PROGRAM ELEMENT, PROJECT, TASK AREA & WORK UNIT NUMBERS
11. CONTROLLING OFFICE NAME AND ADDRESS Advanced Concepts Branch (AFWL-NTYP) Air Force Weapons Laboratory Kirtland AFB, New Mexico 87117		12. REPORT DATE December 1981
		13. NUMBER OF PAGES 62
14. MONITORING AGENCY NAME & ADDRESS (if different from Controlling Office)		15. SECURITY CLASS. (of this report) Unclassified
		15a. DECLASSIFICATION/DOWNGRADING SCHEDULE
16. DISTRIBUTION STATEMENT (of this Report)  Approved for public release; distribution unlimited		
17. DISTRIBUTION STATEMENT (of the abstract entered in Block 20, if different from Report)		
18. SUPPLEMENTARY NOTES  Approved for public release; IAW AFR 190-17  FREDERIC C. LYNN, Major, USAF Director of Public Affairs  J. S. Wolan Dean for Research and Professional Development		
19. KEY WORDS (Continue on reverse side if necessary and identify by block number) Insulator Flashover Gap Closure Ablative Surface Soft Photon Power Flow		Air Force Institute of Technology (ATC) Wright-Patterson AFB, OH 45433
20. ABSTRACT (Continue on reverse side if necessary and identify by block number) Understanding the physical processes of high power electrical energy is of major importance for the advancement of state-of-art directed energy, simulation, and confined fusion programs. Generation of high voltage, short duration pulses may result in high energy density plasma which produces quantities of VUV and soft X-ray photons in the range of 0.5-10 ev. Power transport down vacuum lines presents two problems which must be dealt with in every application- insulator flashover and electrode gap closure. The pulsed flashover and ablative closure mechanisms under soft VUV photon fluence are described. Two		

DD FORM 1 JAN 73 1473

EDITION OF 1 NOV 65 IS OBSOLETE

UNCLASSIFIED

SECURITY CLASSIFICATION OF THIS PAGE (When Data Entered)



UNCLASSIFIED

SECURITY CLASSIFICATION OF THIS PAGE(When Data Entered)

tests were conducted. First, an insulator surface was subjected to VUV photons (0.5 ev) using apertures of 0.0156 to 0.5 inches in diameter with and without a quartz window. The apertures had no effect in inhibiting a flashover; however, the quartz window prevented the occurrence of insulator flashover. Second, the gap closure rate of copper electrodes under the photon fluence of  $6 \times 10^9$  watts per square meter was measured. A gap closure rate of 0.35 cm/microsecond was determined for the copper electrodes.

UNCLASSIFIED

SECURITY CLASSIFICATION OF THIS PAGE(When Data Entered)

DATE  
FILMED  
7-8